JACS
JOURNAL OF THE AMERICAN CHEMICAL SOCIETY

ARTICLE

pubs.acs.org/JACS

The Surface Trans Effect: Influence of Axial Ligands on the Surface Chemical Bonds of Adsorbed Metalloporphyrins

Wolfgang Hieringer,*[,†] Ken Flechtner,[‡] Andreas Kretschmann,[‡] Knud Seufert,[§] Willi Auwärter,[§] Johannes V. Barth,[§] Andreas Görling,[†] Hans-Peter Steinrück,[‡] and J. Michael Gottfried*[,‡]

[†]Lehrstuhl für Theoretische Chemie, Universität Erlangen-Nürnberg, Egerlandstrasse 3, 91058 Erlangen, Germany

[‡]Lehrstuhl für Physikalische Chemie II and Interdisciplinary Center for Molecular Materials (ICMM), Universität Erlangen-Nürnberg, Egerlandstrasse 3, 91058 Erlangen, Germany

[§]Physik-Department E20, Technische Universität München, James-Franck-Strasse, 85748 Garching, Germany

Supporting Information

ABSTRACT: The chemical bond between an adsorbed, laterally coordinated metal ion and a metal surface is affected by an additional axial ligand on the metal ion. This surface analogon of the *trans* effect was studied in detail using monolayers of various M(II)-tetraphenylporphyrins (MTTPs, M = Fe, Co, Zn) and their nitrosyl complexes on a Ag(111) surface. X-ray photoelectron spectroscopy (XPS) shows that the oxidation state of the Fe and Co (but not Zn) ions in the MTPP monolayers is reduced because of the interaction with the substrate. This partial reduction is accompanied by the appearance of new valence states in the UV photoelectron and scanning tunneling spectra (UPS and STS), revealing the covalent character of the ion-substrate bond. Subsequent coordination of nitric oxide (NO) to the metal ions (Fe, Co) reverses these surface-induced effects, resulting in an increase of the oxidation states and the disappearance of the new valence states. Removal of the NO ligands by thermal desorption restores the original spectroscopic features, indicating that the described processes are fully reversible. The NO coordination also changes the spin state and thus the magnetic properties of the metal ions. Density-functional theory (DFT) calculations on model systems provide structural and energetic data on the adsorbed molecules and the surface chemical bond. The calculations reveal that competition effects, similar to the *trans* effect, play a central role and lead to a mutual interference of the two axial ligands, NO and Ag, and their bonds to the metal center. These findings have important implications for sensor technology and catalysis using supported planar metal complexes, in which the activity of the metal center is sensitively influenced by the substrate.

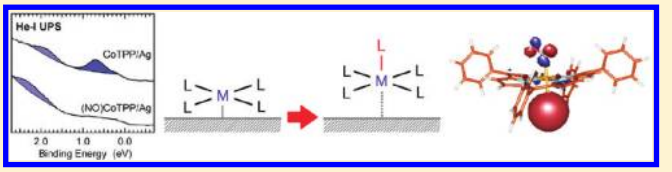

1. INTRODUCTION

Adsorbed metal complexes are promising candidates for novel heterogeneous catalysts with well-defined active sites. The uniform reactivity of these sites ensures a similarly high selectivity as known from homogeneous catalysts, while the practical advantages of heterogeneous catalysts are maintained.[1−7] Another important application of adsorbed complexes is the sensing of gases, in which the coordination of gas molecules to the metal center causes measurable changes of electronic properties, color, etc.[8−12] Planar complexes such as metalloporphyrins and -phthalocyanines are particularly well suited for anchoring on solid substrates, because they readily form ordered monolayers by self-assembly[13−28] and possess two axial coordination sites available as centers of catalytic activity or sensor functionality.

This coordinatively unsaturated character of the metal ions is the key to the specific reactivity and the biological importance of metalloporphyrins in a large number of enzymes. For example, in heme-thiolate proteins, such as the cytochrome P450 family, the active center consists of an iron porphyrin with an axial thiolate ligand, which influences the electronic structure and facilitates the O−O bond cleavage and other reactions.[29] In the case of adsorbed metal complexes, the substrate can operate as an additional ligand to the metal center and thus play a similar role as the thiolate ligand for the Fe center in the cytochrome P450 enzymes.[30] For example, cobalt tetraphenylporphyrin (CoTPP) on TiO_2 catalyzes the reduction of NO_x with H_2 or CO, while unsupported CoTPP or TiO_2 alone are inactive. The activity enhancement is apparently related to electron transfer from the oxide to the Co ion, as was deduced from investigations of $CoTPP/TiO_2$ powder samples with UV and EPR spectroscopy.[6,7] Other support materials have a similar influence on the activity of Co porphyrins; for example, thiol-functionalized Co porphyrin anchored to Au(111) catalyzes the liquid-phase oxidation of hydrochinone to benzochinone with O_2 more efficiently than the unsupported porphyrin.[3] Likewise, Mn porphyrin on Au(111) catalyzes the epoxidation of stilbene, as was observed with scanning tunneling microscopy (STM) on the liquid−solid interface.[1]

These and further observations make a fundamental understanding of the chemical bond between metal complexes and surfaces desirable. This aim requires a detailed investigation of

Received: October 17, 2010
Published: April 04, 2011

dx.doi.org/10.1021/ja1093502 | *J. Am. Chem. Soc.* 2011, 133, 6206–6222

the influence of the surface on the electronic structure of the metal center. Recently, we studied monolayers of CoTPP[30,31] and Co(II)-octaethylporphyrin (CoOEP)[32] on a Ag(111) surface with photoelectron spectroscopy and found a new electronic valence state, which results from a covalent/coordinative interaction between the complexed Co ion and the Ag substrate.[27,30−33] This interaction is accompanied by a transfer of electron density from the Ag surface to the Co ion, as indicated by a substantial shift of the Co(2p) level to lower binding energy.

Previously, it was shown that this Co−Ag interaction is suppressed if a nitric oxide (NO) ligand binds to the coordinated Co ion.[34] This observation was preliminarily interpreted as a manifestation of the *trans effect*, which is an established concept in classical, solution-based coordination chemistry and describes the competition between two ligands in *trans* position binding to the same metal center.[35−39] NO was chosen as a ligand, because it exerts an exceptionally large *structural trans effect*[38] and has found continued interest as a ligand to adsorbed tetrapyrrole complexes.[40−43] Due to the *trans* effect, a ligand can modify the metal-to-ligand (M−L) bond of other ligands within a complex. In particular, it can weaken the M−L bond of the ligand in *trans* position or, in other words, two *trans* ligands compete for the stronger bond to the metal center. Typical manifestations of this effect are the increased M−L bond length of the "weaker" *trans* ligand (*structural trans effect*) and the increased kinetic lability of the weaker ligand toward substitution (*kinetic trans effect*). "Strong" ligands with a very high *trans activity*, such as NO^-, N^{3-}, O^{2-} and S^{2-}, induce large structural *trans* effects in octahedral and square-planar complexes. H^-, R^-, RCO^- and RN_2^- also show substantial *trans* activity, while the ligands CO, CN^-, NO_2^-, PR_3 and RS^- are relatively "weak".[38]

The observation of a *trans* effect on adsorbed complexes under participation of the substrate acting as an axial ligand is very important with respect to catalysis on supported metal complexes, because it reveals how a coordinated reactant molecule alters the properties of the active site. Therefore, a detailed investigation of chemical bonding and electronic interactions of reactive adsorbed metal complexes must take these ligand- and surface-induced effects explicitly into account. This is the focus of the present work, which reports a joint experimental and theoretical investigation of the chemical bond between complexed metal ions (Fe, Co) and a Ag(111) surface and the influence of an axial NO ligand on this bond. These more reactive systems will be compared to complexed Zn ions in a similar environment as a relatively inert counterpart and data of the interaction of ZnTPP/Ag(111) with an NH_3 ligand.

2. EXPERIMENTAL AND COMPUTATIONAL DETAILS

2.1. Photoelectron Spectroscopy (PES). All PES investigations were performed with a *Scienta* ESCA-200 photoelectron spectrometer which was described in detail elsewhere.[32] The sample was a discoidal Ag single crystal (purity >99.999%) with a polished (111) surface, which was aligned to <0.1° with respect to the nominal orientation (see ref.[31] for details about sample preparation). Two type K thermocouples were mounted to the rim of the Ag crystal for temperature measurement (±5 K). The crystal was attached to a manipulator with facilities for cooling and heating in the temperature range 95−900 K.

UP spectra were taken with He−I radiation (21.22 eV) and a sample bias of −10 V. The reported XPS and UPS binding energies are referenced to the Fermi edge of the clean Ag surface ($E_B \equiv 0$). The following photoelectron detection geometries were used: All UP spectra and the XP spectra (A) and (C) in Figure 1 were recorded in normal emission; the other XP spectra were collected in grazing emission (80° with respect to the surface normal) for increased surface sensitivity.

5,10,15,20-Tetraphenylporphyrin (2HTPP) and its metal complexes zinc(II)-tetraphenylporphyrin (ZnTPP) and cobalt(II)-tetraphenylporphyrin (CoTPP) (purity >98%) were degassed *in vacuo* for 24 h at 420 K prior to use and evaporated with a Knudsen cell at 638 K. The resulting flux of typically 0.05 Å/s at the sample position was measured with a quartz crystal microbalance. Monolayers of CoTPP and ZnTPP were prepared by deposition of CoTPP and ZnTPP multilayers, respectively, followed by thermal desorption of the excessive multilayers at 550 K as explained in refs.[31,44] For the preparation of iron(II)-tetraphenylporphyrin (FeTPP) monolayers, 2HTPP monolayers (prepared as described above for CoTPP and ZnTPP, cf. refs.[31,45]) were metalated directly on the surface by deposition of the stoichiometric amount of Fe atoms as described in refs.[19,20,45−47]

For the preparation of the monolayers of (NO)CoTPP and (NO)FeTPP, NO gas (>99.5%) was dosed onto CoTPP and FeTPP monolayers, respectively, with a pressure of 3×10^{-8} mbar at a sample temperature of 140 K. The total NO dosage was 300 L (Langmuir, 1 $L = 1 \times 10^{-6}$ Torr × s). No direct adsorption of NO on the Ag(111) surface was observed under these conditions.[48] (NO)CoTPP multilayers were prepared by dosing NO (3×10^{-8} mbar) during the vapor deposition of CoTPP at 140 K (total NO dosage: 800 L). The XP and UP measurements on (NO)CoTPP and (NO)FeTPP were performed at 140 K at an NO pressure of 3×10^{-8} mbar.

The coverage θ is defined as the number of adsorbed molecules or atoms divided by the number of substrate atoms, whereas the term "monolayer" denotes a complete, saturated adlayer of molecules in direct contact with the substrate surface at 300 K. Monolayer coverage corresponds to $\theta = 0.037$.[31]

2.2. Scanning Tunneling Spectroscopy. The scanning tunneling spectroscopy (STS) and microscopy (STM) experiments were performed in a custom-designed, stand-alone ultrahigh vacuum (UHV) apparatus[49] comprising a commercial low-temperature STM.[50] The system base pressure is below 2×10^{-10} mbar. All ST spectra were recorded under open feedback loop conditions via lock-in technique using electrochemically etched tungsten tips. The STM images were taken in constant current mode. For STM and STS measurements, the sample was kept at 6 K. Submonolayer coverages of CoTPP and in situ metalated FeTPP were applied in order to have bare Ag(111) patches available to characterize the tip electronic structure prior to any experiment. In the figure caption, V refers to the bias voltage applied to the sample. While the general experimental procedures were followed as described in Section 2.1, we applied lower NO doses (around 10 L) to not fully saturate the metallotetraphenylporphyrin (MTPP) layers. This allows for a direct spectroscopic comparison of NO/MTPP and MTPP with an identical tip.

2.3. Computational Methods. All quantum-chemical calculations presented here are based on density-functional theory (DFT).[51,52] Both periodic and nonperiodic calculations were performed to study two different types of model systems that, in a complementary way, describe different aspects of the experimental system. As the first type of model systems, periodic slab calculations of metalloporphyrin (MP) molecules adsorbed on a Ag(111) surface slab have been performed using the Vienna Ab Initio Simulation Package (VASP).[53] For the second type of model systems, nonperiodic calculations on isolated MTPP complexes coordinated to a single Ag atom or a cluster of Ag atoms were carried out. For the geometry optimizations of these systems, the Turbomole[54] program package was used in most cases. For the analysis of the electronic structure, the ADF[55] program was employed. The calculations were performed in the spin-unrestricted framework, and care was taken that the lowest-energy spin state was attained.

For the periodic slab calculations, the tetraphenylporphyrins investigated in the experiments have been simplified to the corresponding

basic porphins, that is, the peripheral phenyl groups have been replaced by hydrogen atoms. While these metalloporphins are not expected to quantitatively reproduce all properties of the MTPP complexes used in the experiments, they feature reduced steric repulsions of the ligand with the metal surface and hence allow us to isolate the electronic *trans* effect analogon which is central to this study. An orthorhombic unit cell of the size $14.4 \times 15.0 \times 35.4$ Å^3 has been used. The unit cell contained a single metalloporphin (MP) molecule (M = Co, Fe) plus a five-layer Ag slab with a total of 150 Ag atoms. This unit cell implies a vacuum layer of approximately 18 Å, which serves to decouple the individual slabs in the vertical dimension. The MP molecules have been placed on the Ag(111) surface such that the central metal M was next to a top-site Ag atom (Ag_{top}) of the silver surface. Test calculations revealed that adsorption over a bridge site or an fcc hollow site of the Ag(111) surface are associated with similar binding energies (within about 0.1 eV) at the present theoretical level. We chose top-site adsorption for our analysis in order to allow for a direct comparison with model Ag complexes. Details of the final geometries can be found in the Supporting Information (SI). In all geometry optimizations involving the Ag slab the two topmost layers of the slab were fully relaxed, while the bottom three layers were kept fixed at the bulk positions of an fcc Ag crystal. All other atomic positions have been optimized without constraints until the energy gradients dropped below 5×10^{-3} eV/Å. The PBE generalized gradient approximation (GGA) functional due to Perdew, Burke and Ernzerhof[56] has been used unless stated otherwise, and the projector-augmented wave method (PAW)[57,58] has been employed to treat the atomic cores. The "normal" precision setting was used in the VASP calculations, which corresponds to a global plane-wave energy cutoff of 400.0 eV (29.40 Ry, 5.42 au). A single k-point has been used for the unit cell described above (5×6 Ag atoms per layer). We have checked our results against a $3 \times 3 \times 1$ k-point mesh for some cases, but found that the main results were not affected. The convergence criterion for the self-consistent field procedure for the electronic wave functions was set to 10^{-5} eV. All calculations have been carried out in a spin-polarized fashion; the minority spin channel is labeled β in this work. Core level shifts have been estimated from the local average electrostatic potential at each ion following a standard procedure for the periodic calculations.

In general, most GGA density functionals (including those used here) are too repulsive in the long-range dispersion regime, which makes bond energies and bond distances beyond the covalent regime unreliable. In some explicitly indicated cases, we have therefore included an empirical long-range dispersion correction to account for the effect of van der Waals forces (labeled PBE+vdW for the PBE functional with van der Waals dispersion correction).[59] In most cases, however, we have not included any dispersion correction to the standard GGA functional, because we are predominantly interested in the electronic (i.e., covalent or coordinative) interaction of the M(TP)P molecules with the surface, which is usually well described by common GGA functionals. In general, the inclusion of van der Waals dispersion reduces the molecule-surface distances somewhat due to the attractive nature of the interaction.

For the nonperiodic calculations on isolated MTPP complexes using Turbomole and ADF, the exchange-correlation functionals due to Becke[60] and Perdew[61] (hereafter denoted BP) and due to Perdew, Burke and Ernzerhof (PBE)[56] were used. Note that we prefer the BP functional in the study of the molecular model complexes rather than the PBE functional which is used for the periodic density functional calculations. The BP functional has been found suitable for the study of molecular coordination compounds in many previous studies. For the Turbomole and ADF calculations the TZVP and TZ2P basis set[62] and TZ2P have been used, respectively. The influence of metal coordination to the MTPPs was studied by attaching a Ag atom or a small cluster of varying size (Ag_{19}, Ag_{72}) to the metal center (Co, Fe, or Zn) of the metalloporphyrins. For complexes bearing larger Ag clusters (Ag_{19}, Ag_{72}), only a double-ζ basis set (Ahlrich's SV(P) basis set) was employed for better efficiency. For the Turbomole calculations, the resolution-of-the-identity (RI)[63] technique for the Coulomb integrals and its multipole-accelerated version (MARIJ)[64] was used throughout. A similar density-fitting scheme is used by ADF.[65] Full (unconstrained) geometry optimizations were performed in general (using Turbomole), and the minima was confirmed by frequency calculations. For the larger clusters, constraints were used during the geometry optimizations to ensure that the clusters can be regarded as cutouts from the Ag fcc bulk structure. In these cases, relaxation was allowed for those Ag atoms which are involved in the bonding to the metalloporphyrins (see the SI for further details). Additional calculations, especially the fragment orbital based analysis of the electronic structure, have been performed with the help of ADF.

The geometric and electronic structures were subsequently used for the interpretation of the XPS, UPS and STS data using the same exchange-correlation functionals and basis sets. For the nonperiodic calculations, the so-called *Slater transition state*[51,66,67] method to calculate shifts in core ionization potentials was used, and the results were compare with experimental XPS peak shifts[68,69] in order to verify the validity of the computational model systems. Partial charges according to the Bader scheme[70] were used in this study to estimate the direction of charge transfer upon adsorption and ligand coordination (see the SI for details). The densities for the Bader partitioning were obtained from the periodic calculations as described above.

3. EXPERIMENTAL RESULTS

3.1. X-Ray Photoelectron Spectroscopy (XPS). The central aim of this work is to explore the influence of the Ag surface, of the NO ligand, and of the combination of both on adsorbed, complexed metal ions. For this purpose, we studied monolayers and multilayers of metallo-tetraphenylporphyrins (MTPP, M = Co, Fe, Zn) and their nitrosyl complexes ((NO)MTPP, M = Co, Fe), using the M($2p_{3/2}$) core level signals as a monitor of the ligand-induced changes (Figures 1−3).

Figure 1a shows the Co($2p_{3/2}$) signal of CoTPP multilayers, that is, a system in which the majority of the molecules does not interact with the Ag substrate. The maximum is located at 780.0 eV, which is typical of cobalt in a formal +2 oxidation state and agrees with the nominal oxidation state of the ion. The multiplet structure of the signal is caused by the unpaired electron of the Co(II) ion (d^7).[31]

The Co($2p_{3/2}$) signal of the CoTPP monolayer (Figure 1b) has its maximum at 778.2 eV and also shows a multiplet structure. The chemical shift of −1.8 eV relative to the multilayer signal exceeds by far the respective surface-induced core-level shifts for the other elements, carbon (−0.2 eV) and nitrogen (−0.3 eV), as was discussed previously.[31] While these small shifts of the C(1s) and N(1s) signals can be attributed to final state effects (relaxation shift), the much larger shift of the Co(2p) signal suggests operation of initial state effects, such as transfer of electron density from the Ag surface to the Co ion. This assumption is supported by the theoretical analysis, which indicates a charge transfer of 0.37e from the surface to cobalt porphin (cf. Section 2.3 and the SI for details; additional evidence (not shown) is given by the calculated (initial-state) N 1s orbital energies or core-potential shifts upon Ag or Ag(111) coordination, which are very small (<0.3 eV)). The shoulder around 778 eV in the Co($2p_{3/2}$) multilayer spectrum (Figure 1a) arises from molecules in the first layer, since its intensity depends on the thickness of the multilayer and eventually vanishes for thick multilayers.

The Co($2p_{3/2}$) signal of (NO)CoTPP multilayers (Figure 1c) shows how the NO ligand influences Co ions that do not interact with the Ag surface. Comparison to the multilayer signal of CoTPP reveals two major differences: First, the maximum is shifted to higher binding energy by +0.8 eV and second, the multiplet structure vanished. The positive peak shift indicates a partial oxidation of the Co ion by the NO ligand,

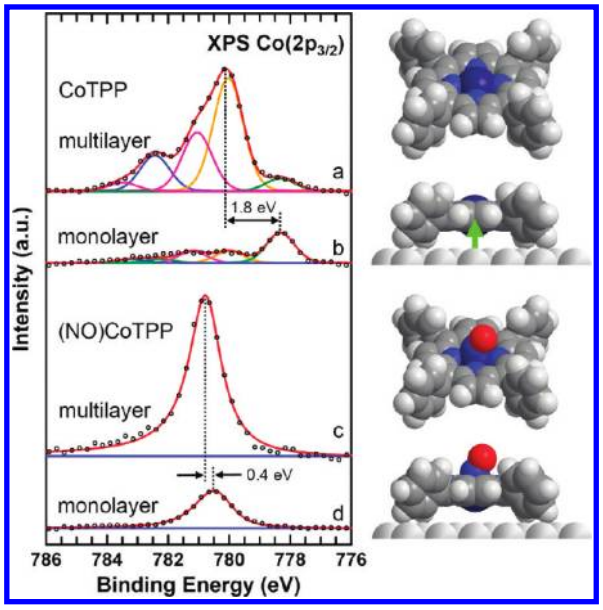

Figure 1. $Co(2p_{3/2})$ XP spectra of CoTPP and (NO)CoTPP on Ag(111): (a) CoTPP multilayers (~4 layers), (b) CoTPP monolayer, (c) (NO)CoTPP multilayers (~4 layers), and (d) (NO)CoTPP monolayer. The small shoulder around 778 eV in (a) stems from the CoTPP monolayer. The other curves in the signal deconvolution of (a) and (c) are displayed for illustrative purposes and do not necessarily represent the full complexity of the spectra.

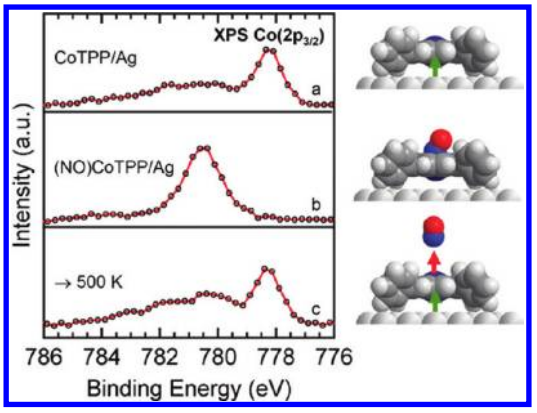

Figure 2. Reversibility of the changes in the electronic structure induced by NO coordination: $Co(2p_{3/2})$ XP spectra of CoTPP and (NO)CoTPP on Ag(111). (a) CoTPP monolayer, (b) (NO)CoTPP monolayer, (c) after heating the (NO)CoTPP monolayer to 500 K for thermal desorption of the NO ligand.

which in turn acquires a partial anionic (nitroxylic) character. (The theoretical analysis suggests a negative charge of 0.2e on the coordinated NO ligand, see the SI for details.) The multiplet splitting disappears presumably because, upon formation of the NO−Co bond, the spin of the unpaired electron of the NO molecule compensates the spin of the Co(II) ion. Indeed, our own DFT calculations and previous results[71] favor a low-spin (singlet) state for (NO)CoTPP, as will be discussed in detail below.

In the (NO)CoTPP monolayer, the Co ion interacts with two axial "ligands": the NO molecule and, in a *trans* position to it, the Ag surface. The related $Co(2p_{3/2})$ spectrum in Figure 1d shows a single peak shifted by −0.4 eV compared to the (NO)CoTPP multilayer signal. This is only slightly more than the relaxation shifts of the C(1s) (−0.2 eV) and

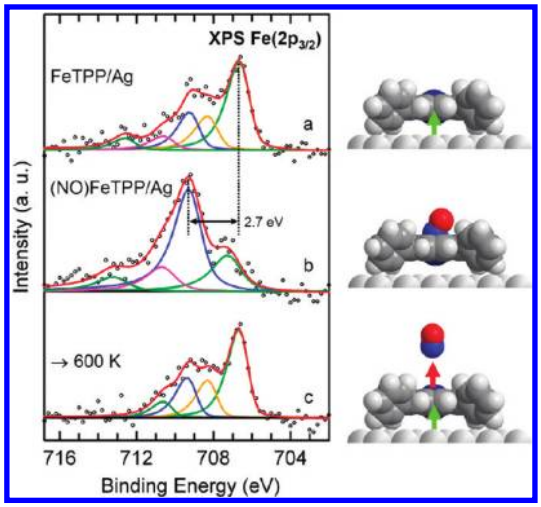

Figure 3. Coordination of NO to a FeTPP monolayer on Ag(111) and thermal desorption of the NO ligand, $Fe(2p_{3/2})$ XP spectra: (a) FeTPP monolayer, (b) (NO)FeTPP monolayer, (c) after heating the (NO)FeTPP monolayer to 600 K.

N(1s) (−0.3 eV) signals and much less than the $Co(2p_{3/2})$ shift of −1.8 eV between multilayer and monolayer CoTPP in the absence of the NO ligand. Obviously, it makes little difference whether the (NO)CoTPP complex is in contact to the surface or not, suggesting that the Co−Ag interaction is reduced by the NO ligand. This conclusion is confirmed by the UPS, STS, and DFT results discussed below.

Figure 2 illustrates that the suppression of the Co−Ag interaction is fully reversible: heating of the (NO)CoTPP monolayer to 500 K removes the NO ligand and restores position and shape of the original $Co(2p_{3/2})$ signal prior to NO coordination on the Co ion.

Similar observations were made for FeTPP. Figure 3a shows the $Fe(2p_{3/2})$ signal of the FeTPP monolayer with a main peak at 706.7 eV and a complex multiplet structure, which is attributed to the open-shell character of the Fe(II) ion. (The present and earlier[72] DFT calculations predict indeed a triplet ground state for isolated FeTPP, see below). Formation of (NO)FeTPP by coordination of NO to the FeTPP monolayer (Figure 3b) shifts the maximum of the $Fe(2p_{3/2})$ signal by +2.7 to 709.4 eV. In analogy to (NO)CoTPP, this large shift toward higher binding energy is interpreted as an NO induced suppression of the Fe−Ag interaction. Part of the shift may also be attributed to a partial oxidation of the Fe ion by the NO ligand (see the discussion in the next paragraph and the SI for calculated partial charges). In contrast to (NO)CoTPP, the (NO)FeTPP monolayer signal still shows multiplet structure, reflecting the complex electronic structure of the Fe ion in a porphyrin complex.[73] Due to the additional unpaired electron from the NO ligand, the Fe ion probably changes from the triplet state as the lowest-energy state[73,74] to a doublet or quartet state. Which of these states dominates cannot be decided on the basis of our XP spectra; however, our DFT calculations predict a doublet ground state, see below. In addition, Figure 3b shows good agreement with spectra of other Fe(III) complexes.[75] As was the case for the (NO)CoTPP complex, thermal desorption of the NO ligand restores the original spectrum within the noise limit, that is, the described effects are reversible also for the FeTPP system (Figure 3c). The NO ligand is apparently stronger bound than in the Co complex, since a temperature of 600 K is necessary for its desorption.

The FeTPP monolayers were prepared by direct metalation of 2HTPP monolayers on Ag(111) with the stoichiometric amount of vapor-deposited Fe as described in Section 2.1.[19,20,47] This in situ approach was chosen because of the high sensitivity of FeTPP toward oxidation, which makes preparation and handling outside the vacuum

dx.doi.org/10.1021/ja1093502 |J. Am. Chem. Soc. 2011, 133, 6206–6222

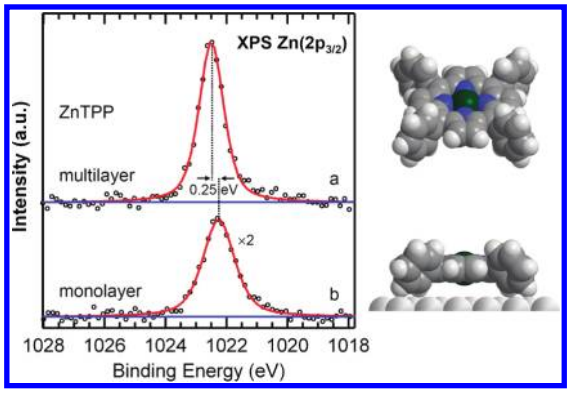

Figure 4. $Zn(2p_{3/2})$ XP spectra of (a) multilayers and (b) monolayer of ZnTPP on Ag(111).

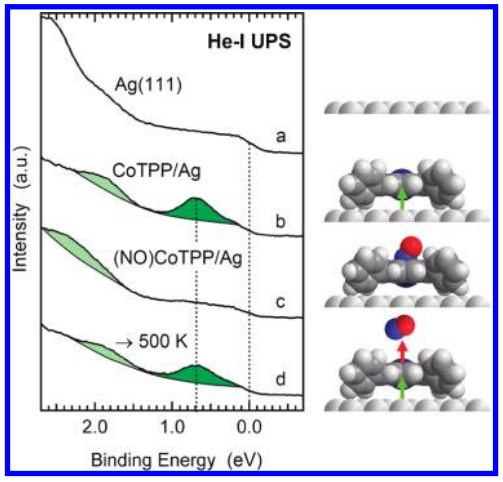

Figure 5. Manifestations of the surface coordinative bond in the valence electronic structure and the influence of the NO ligand on the Co−Ag interaction in CoTPP monolayers on Ag(111): He−I UP spectra ($h\nu$ = 21.22 eV) of (a) clean Ag(111) surface, (b) CoTPP monolayer, (c) (NO)CoTPP monolayer, and (d) after heating the (NO)CoTPP monolayer to 500 K for thermal desorption of the NO ligand.

difficult.[76] While yielding high degrees of metalation in the monolayer (>90%), this method is less efficient for the metalation of multilayers, because only a fraction of the Fe atoms deposited is coordinated by the 2HTPP multilayers. Since the remaining part of the Fe retains the ±0 oxidation state, probably by formation of Fe clusters,[20] comparison with pure FeTPP and (NO)FeTPP multilayers is not possible here. However, we can compare with multilayers and monolayers iron(II) phthalocyanine (FePc), which have been studied previously and in which Fe has a very similar coordination environment.[77] The $Fe(2p_{3/2})$ signal of FePc multilayers shows a broad multiplet structure around 708.8 eV. In the FePc monolayer signal, the maximum is shifted by −1.7 to 707.2 eV, while the signal shape is very similar to Figure 3a. This comparison suggests that the larger part (+1.7 eV) of the NO-induced shift of +2.7 eV is caused by the suppression of the Fe−Ag interaction, while a smaller part (+1.0 eV) is due to electron transfer from the Fe ion to the NO ligand.[78] This implies that the NO ligand has predominantly anionic (NO^-) character (cf. the SI for calculated partial charges).

The close similarities in the interaction of Co and Fe ions with the Ag surface and toward the coordination of NO may suggest that other complexed transition metal ions in proximity to a metal surface may behave similarly. This, however, is not generally the case, as is illustrated

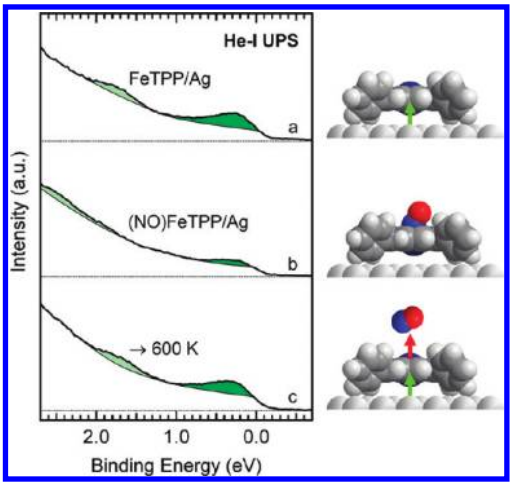

Figure 6. Valence electronic structure of FeTPP and (NO)FeTPP on Ag(111): He−I UP spectra of (a) FeTPP monolayer, (b) (NO)FeTPP monolayer, and (c) after heating the (NO)FeTPP monolayer to 600 K for removal of the NO ligand.

by Figure 4, which shows the $Zn(2p_{3/2})$ signal of multilayers and monolayer of ZnTPP on Ag(111). The peak positions differ here by only 0.25 eV, which is in the same range as the C(1s) and N(1s) core level shifts and probably largely due to relaxation. Apparently, there is little or no electronic interaction between the Zn(II) ion and the Ag surface. This interpretation is supported by the UP spectra and the computational results discussed below. Unsurprisingly, the coordination of a ligand (here NH_3, since no nitrosyl ligation was observed) to the Zn ions of a ZnTPP monolayer causes only a small shift of the $Zn(2p_{3/2})$ level, −0.2 eV, and the Zn−NH_3 bond is relatively weak (desorption of NH_3 around 150 K).[79] The binding energy of NH_3 to gas-phase ZnTPP is computed to 49 kJ/mol (BP/TZVP density-functional level), which is in good agreement with experiment where a Zn−NH_3 bond dissociation energy of 40 kJ/mol was estimated.[79]

3.2. UV Photoelectron Spectroscopy (UPS). In this section, we focus on the influence of the Ag surface and the NO ligand on the valence electronic structure of the metal complexes. The He−I UP spectra (a) and (b) in Figure 5 refer to the clean Ag(111) surface and to a monolayer of CoTPP on Ag(111), respectively. As previously shown, the signal around 0.6−0.7 eV in Figure 5b results from the electronic interaction of the coordinated cobalt ion with the Ag surface.[31] This signal was tentatively attributed to the interaction of Co 3d orbitals with electronic states of the porphyrin macrocycle and the Ag surface.[31,33] It was proposed that this interaction leads to two new electronic states, which are located below the Fermi energy (E_F) of Ag and thus are populated by electrons from the substrate. Therefore, this model suggests transfer of electron density from the surface to the Co ion and is thus in agreement with the XPS results discussed above. (This tentative model is analyzed in more detail using our DFT calculations, as will be explained below.) Upon coordination of NO to the Co ion (Figure 5c), the interaction-induced signal around 0.6−0.7 eV disappears and the signal around 2 eV shifts by +0.4 eV, reaching the position of the highest occupied state of a CoTPP multilayer.[31] These changes are reversed when the NO ligand is removed by heating to 500 K (Figure 5d).

Figure 6 shows the analogous results for FeTPP. The interaction-induced peak (Figure 6a, marked in green) is here located slightly below E_F and is less intense than in the case of CoTPP. Its intensity is strongly reduced by coordination of NO to the Fe ion (Figure 6b) and restored upon thermal desorption of the NO ligand by heating to 600 K (Figure 6c).

dx.doi.org/10.1021/ja1093502 |J. Am. Chem. Soc. 2011, 133, 6206–6222

For both CoTPP and FeTPP, the NO-induced changes in the valence region are consistent with the conclusion drawn from the XPS data: Both sets of UP spectra show that the central metal ions in (NO)MTPP monolayers (M = Co, Fe) are far less influenced by the Ag surface than in MTPP monolayers. In other words, coordination of the NO ligand weakens the interaction of the metal ion with the substrate.

The interaction of ZnTPP with the Ag surface does not lead to significant changes of the valence electronic structure, as can be seen in Figure 7, which compares monolayer UP spectra of ZnTPP, CoTPP, FeTPP, and 2HTPP. Between E_F and 1.5 eV, the ZnTPP spectrum is almost identical to the spectra of the 2HTPP monolayer and of the pure Ag surface (cf. Figure 5a). In contrast, the spectra of CoTPP and FeTPP show the interaction-induced signals described above. The relative inertness of ZnTPP is attributed to the completely occupied Zn(3d) levels and their low energies (i.e., high binding energies).[80] In addition, monolayer and multilayers of ZnTPP show very similar UP spectra; no additional signals appear in the monolayer spectrum. A table with all valence peak positions of ZnTPP and CoTPP monolayers and multilayers and of the FeTPP monolayer is reproduced in the SI (Table S1). Coordination of NH_3 to the Zn ion[79] does not lead to significant changes in the UP spectra in the range between E_F and 3.5 eV (Figure S3 of the SI). This is consistent with the low tendency of ammonia to bind to ZnTPP as predicted by our DFT calculations (see below).

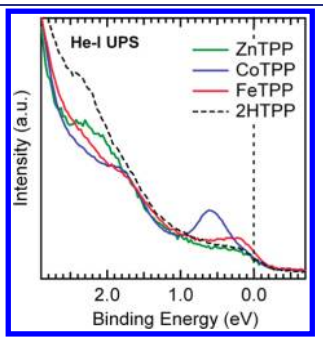

Figure 7. Comparison of the He−I UP spectra of CoTPP (blue), FeTPP (red), ZnTPP (green), and 2HTPP (black, dashed).

3.3. Scanning Tunneling Spectroscopy (STS). Up to now we reported results on the valence electronic structure of MTPP molecules on Ag(111) gained by spatially averaging photoemission experiments for occupied states. In this section, we compare these findings with spectroscopic data acquired on the single molecule level by scanning tunneling spectroscopy (STS). Besides being a local probe, STS has the advantage to yield information also on unoccupied levels above E_F. Figure 8 shows scanning tunneling microscopy (STM) images of CoTPP (Figure 8a) and FeTPP (Figure 8b) species with and without coordination of an additional NO ligand, together with the corresponding ST spectra (Figure 8c and d, respectively). A detailed discussion of the STM images is beyond the scope of this article, but it should be noticed that bare MTPP molecules[27] can be clearly discriminated from the (NO)MTPP species. All the spectra presented in Figure 8c and d are recorded at an identical off-center position above the porphyrin macrocycle (see Figure 8a and b). This location was chosen to maximize the contribution

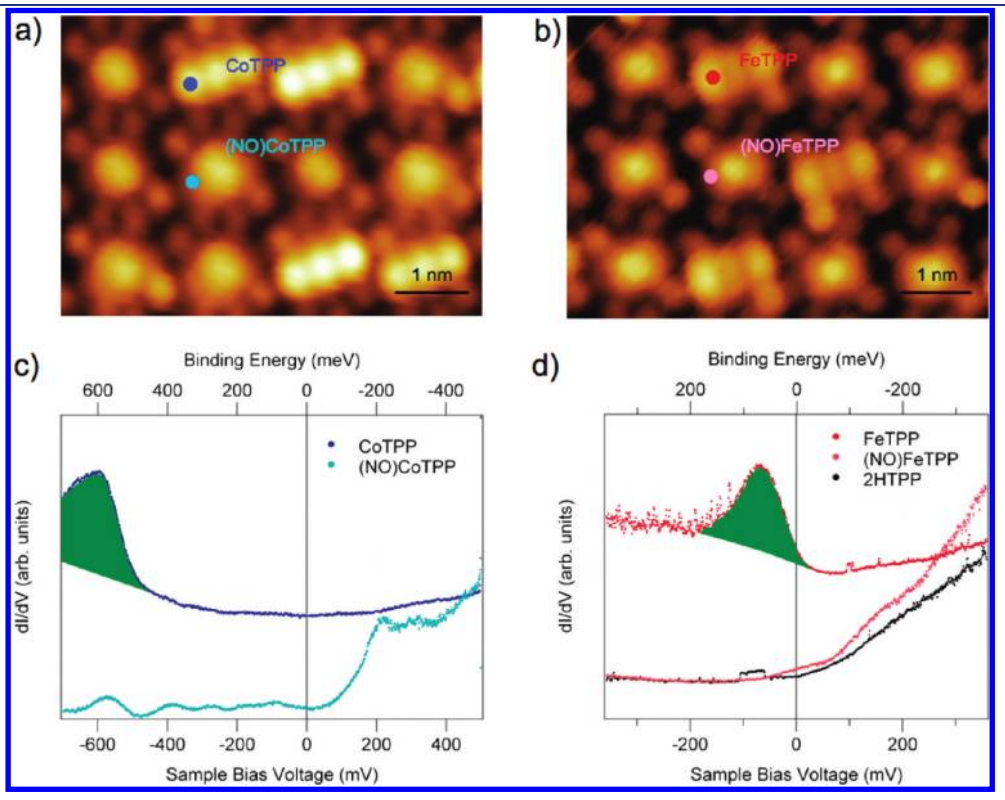

Figure 8. Scanning tunnelling microscopy (STM) images and ST spectra of MTPP and (NO)MTPP on Ag(111) showing the quenching of the interaction-induced peak (marked in green) upon NO coordination. (a) STM image of a mixed CoTPP and (NO)CoTPP array (I = 55 pA, V = −0.7 V). The NO related species are characterized by a round central protrusion. The colored dots represent the off-center position above the porphyrin macrocycle where ST spectra were recorded (compare c and d), see text for discussion). (b) Mixed FeTPP and (NO)FeTPP array (I = 0.1 nA, V = −0.7 V). (c) ST spectra of CoTPP (blue) and (NO)CoTPP (light blue), compare to the UP spectra in Figure 5. (Stabilizing parameters for the STM tip before opening the feedback loop: I = 55 pA, V = −0.6 V, modulation amplitude 25 mV, modulation frequency 967 Hz.) (d) ST spectra of FeTPP (red), (NO)FeTPP (light red) and 2HTPP (black) on Ag(111), compare to Figure 6 (I = 0.2 nA, V = −0.28 V, modulation amplitude 25 mV, modulation frequency 398 Hz).

dx.doi.org/10.1021/ja1093502 |J. Am. Chem. Soc. 2011, 133, 6206–6222

of the interaction-induced state.[33] As these spectra are taken on individual molecules, the observed peak width is reduced in comparison to the laterally averaging UP spectra. Addressing first the occupied states of the bare MTPPs, we observe a well-defined peak around 0.6−0.7 eV binding energy (between −0.6 and −0.7 V sample bias) for CoTPP and a similar feature at a binding energy of 0.1 eV for FeTPP. These spectral fingerprints are in full agreement with the UPS data presented in the previous section and represent the interaction-induced state (cf. Figures 5 and 6). Similar occupied resonances were previously reported in STS studies on Co- and Fe-porphyrin molecules in contact with noble metal surfaces.[13,33,81,82] Above the Fermi energy, the curves of the bare MTPPs are featureless in the energy range investigated here. From the theoretical calculations presented in Section 4.3 (Figure 12), we estimate the gap between the bonding and the antibonding orbital to at least 1.7 eV, which means that this antibonding level is above the energy range shown in Figure 8c and d.

Upon coordination of NO to either the Co or Fe center of the MTPPs, the interaction-induced state is completely quenched. The resulting spectra are featureless in the displayed binding energy range below E_F. Thus, the results from UPS are confirmed on a single molecule level. In addition, NO coordination induces an enhanced spectral density above E_F. Both the (NO)CoTPP and the (NO)FeTPP spectra exhibit an increase in intensity around 100 mV above E_F, where the bare MTPP spectra showed no features. On first sight, the additional intensity upon coordination to NO might be explained as originating from the antibonding state suggested in Figures 13 and 14 (see below). However, a comparison of the (NO)MTPP spectra with a spectrum taken on free-base 2HTPP (cf. Figure 8d) shows very close similarities. Accordingly, we suggest that the NO coordination not only reduces the interaction between the MTPP and the underlying Ag(111) substrate, but may also modify the interaction between the central ion's d states and the porphyrin macrocycle. Thus, the electronic structure of NO/MTPP around E_F seems to resemble its free-base 2HTPP counterpart. Based on these STS data, it cannot be decided which part of the spectral density above E_F is related antibonding states of the M−NO interaction and which part is due to a partial decoupling of the metal ion from the surface and from the porphyrin ligand.

4. THEORETICAL ANALYSIS

The experimental data presented in Section 3 suggest pronounced electronic interactions of CoTPP and FeTPP with a Ag(111) surface and indicate significant changes in the electronic structure of the adsorbate system when an NO ligand is coordinated to the metal center. In this section, we present theoretical data on the geometric structures, binding energies, and electronic structure of the adsorbate systems which yield a more complete characterization and qualitative understanding of the bonding mechanism and the surface *trans* effects in these systems. To achieve this goal, we invoke two kinds of theoretical model systems which emphasize different aspects of the system. On the one hand, we present results from periodic density-functional calculations on the simple metalloporphins (MP, M = Co, Fe, Zn), which are adsorbed on an ideal Ag(111) surface. Here, the metal center of the MP molecules has been placed over a top-site of the Ag(111) surface. In the second class of model systems, the coordination of a single Ag atom or small cluster to the MTPP molecules is studied. Both approaches are not expected to fully and quantitatively predict all the properties (such as absolute molecule−surface distances) of the experimental adsorbate system. The periodic metalloporphin models have been chosen such that steric effects are largely eliminated, and hence these models allow us to study the electronic

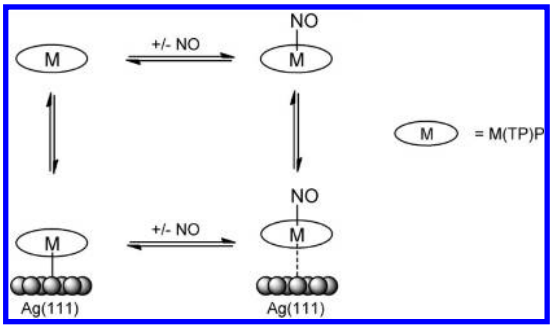

Figure 9. Transformations considered in the theoretical analysis, M = Fe, Co, Zn. In the periodic slab calculations, the MTPP molecules are modeled as metalloporphins MP (i.e., by omitting the peripheral phenyl rings) adsorbed to a five-layer Ag slab (see Section 2 for details). In the molecular model systems, calculations with the full MTPPs have been performed, but the Ag(111) surface has been replaced by a single Ag atom. See Tables 1 and 3 for structural data and Tables 2 and 4 for associated binding energies.

interaction of the complexes with an ideal Ag(111) surface. The second class of models provide additional insight into the changes in the local bonding situation at the metal center upon coordination of the NO ligand and has the advantage that a direct connection to molecular coordination chemistry can be made. We show that the core-level shifts calculated for both of these model systems qualitatively reproduce those observed in the XPS experiments described above (see Table 6 and the SI, Table S2 for details).

The transformations considered in the present computational analysis of both model systems are summarized in Figure 9. For each of the displayed species, geometry optimizations were performed as detailed in Section 2. We start our analysis with a brief discussion of the structural and electronic properties of gas-phase MP and MTPP molecules (in the following summarized as M(TP)P) and then proceed to the effect of Ag coordination.

4.1. Molecular Structures of Metalloporphyrins. The equilibrium and electronic structure of metallotetraphenylporphyrins (MTPP) have been extensively discussed in the literature.[72,83−85] However, most of the early studies considered a highly symmetric geometry (D_{4h} point group), with the peripheral phenyl rings perpendicular to the otherwise completely flat MTPP core structure. It should be noted, however, that such highly symmetric structures in general do not represent the global minimum on the ground-state energy hypersurface, although they may closely approximate it, depending on the central metal M.[72,86,87]

In the doublet ground state of CoTPP, symmetry breaking from D_{4h} symmetry occurs,[87] resulting in a deformation of the initially planar porphyrin core to a saddle shape or twisted saddle structure (D_{2d} or S_4 point group symmetry, respectively). The energy differences between the D_{2d} or S_4 structures (about 3 kJ/mol at the BP/TZVP level) must be considered below the presumed accuracy of the present computational methods, however, and therefore it is best to regard the MTPPs as somewhat flexible, not necessarily completely planar structures. It should be noted that the saddle-shape deformation of the CoTPP core is induced by the peripheral phenyl rings, and the DFT calculations predict a planar minimum structure for the simple, unsubstituted CoP. For the triplet ground state of FeTPP, the lowest-energy conformation features a slightly saddle-shaped TPP core as well. The peripheral phenyl groups are twisted by 69° with respect to the porphyrin plane, resulting in a D_{2d} molecular symmetry. For ZnTPP, we find an almost

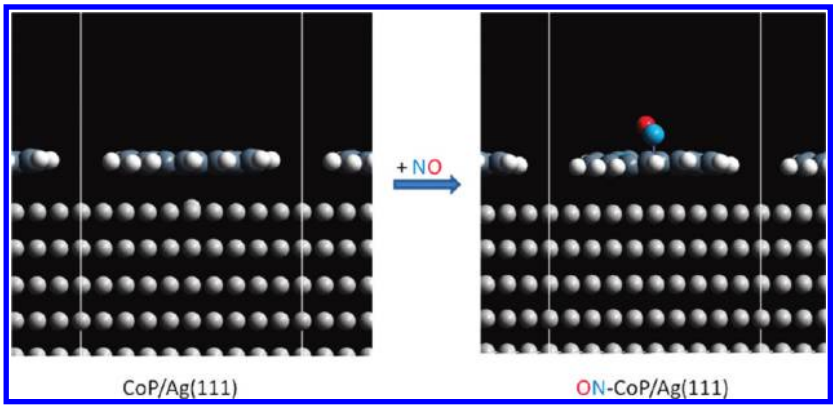

Figure 10. Optimized geometries of the CoP/Ag(111) and (NO)CoP/Ag(111) adsorbate systems from periodic DFT calculations at the PBE+vdW level; geometries for the FeP system are similar; cf. Table 1 for details.

Table 1. Structural Parameters of the CoP, FeP and ZnP Adsorbate Systems Optimized using Periodic Density-Functional Calculations in Angstroms and Degrees[a]

structure	d(M−Ag_{top})	d(M−NO)	d(N−O)	∠(M−N−O)
CoP−Ag(111)	2.88/2.83[b]			
ON−CoP−Ag(111)	>3.5/3.52[b]	1.81	1.19	123
ON−CoP		1.80	1.19	123
FeP−Ag(111)	3.13/2.88[b]			
ON−FeP−Ag(111)	>3.5/3.60[b]	1.71	1.19	145
ON−FeP		1.70	1.19	146
ZnP−Ag(111)	>3.5/3.30[b]			

[a] PBE functional; d(M−Ag_{top}) refers to the distance of M to the top-site Ag atom of the Ag(111) surface. [b] Value including van der Waals correction (PBE+vdW level).

planar TPP core with a very modest saddle shape deformation, and the phenyl rings twisted to an angle of 67° with respect to the porphyrin core (D_{2d} symmetry). More details on the optimized ground state geometries are provided in the SI.

A central point in this study is the nature of the coordinative bond of the central metal ion in MP and MTPP to a Ag surface and the competition with the coordination of an NO ligand in *trans* position. We will first discuss the structural data obtained from our periodic DFT calculations on the MP/Ag(111) adsorbate systems. Illustrations of the optimized geometries are shown in Figure 10, and salient structural data are summarized in Table 1.

4.2. Periodic Systems. CoP adsorbs as a virtually flat molecule, see Figure 10. The total magnetization of the adsorbate system is zero, i.e., it proves to be a nonspinpolarized system. We find a Co−Ag_{top} distance of 2.88 Å at the PBE level (Table 1), which is in the same range as the sum of the covalent radii of both atoms (Co−Ag: 2.71...2.95)[88] and thus suggests a covalent (or coordinative) interaction between the cobalt center and the top-site Ag atom (Ag_{top}) of the surface. It is interesting to note that this top-site Ag atom (i.e., the one closest to the Co center) is slightly lifted above the ideal surface plane toward the Co center by 0.3 Å with respect to its six neighbors in the same plane of the relaxed Ag(111) surface. The binding energy is computed to 54 kJ/mol at the PBE level, that is, without inclusion of dispersion interactions. If van der Waals dispersion is taken into account (PBE+vdW level), the binding energy increases to 275 kJ/mol, and the Co−Ag_{top} distance is reduced by 0.05 to 2.83 Å (Table 1).

Upon coordination of NO to the adsorbed CoP molecule in *trans* position to the Ag surface, the Co−Ag distance increases significantly (cf. Table 1) beyond that of a covalent or coordinative interaction, indicating that the surface covalent bond has been essentially broken. The computed geometry of the now merely physisorbed ON−CoP complex is very similar to the computed geometry of free ON−CoP without the presence of any Ag(111) surface. We estimate the Co−Ag_{top} distance in ON−CoP···Ag(111) to 3.52 Å at the PBE+vdW level, which is 0.69 Å larger than the corresponding Co−Ag_{top} of CoP adsorbed to Ag(111). The total binding energy between NO−CoP and the Ag(111) surface is reduced to 221 kJ/mol including dispersion (only 19 kJ/mol at the PBE level without dispersion correction). In summary, we conclude from the structural and energetic data that CoP is subject to a directed electronic interaction with the Ag(111) surface (top-site), and that this interaction is largely suppressed upon coordination of NO.

The FeP/Ag(111) system is different from CoP/Ag(111) in that the chemical bond between the molecule and the surface is considerably weaker according to our DFT calculations. The binding energy is calculated to only 29 kJ/mol at the PBE density-functional level (excluding van der Waals correction). The optimized Fe−Ag_{top} distance is calculated to 3.13 Å. It is thus considerably larger than the sum of covalent radii (2.77...2.97 Å) and also significantly longer than the corresponding Co−Ag_{top} distance in CoP/Ag(111). Nevertheless, we find a similar elevation of the top-site Ag atom above the Ag(111) plane as was found for the more strongly interacting CoP/Ag(111) system. As expected for such an apparently weak bond, inclusion of the empirical van der Waals correction (PBE+vdW level) results in a smaller Fe−Ag_{top} distance of 2.88 Å, which is, perhaps somewhat surprisingly, similar to the one found for the Co−Ag_{top} distance in the CoP/Ag(111) system. The molecule-surface interaction in FeP/Ag(111) thus appears to be effected by dispersion forces to an even larger extent than in the case of CoP/Ag(111). The corresponding total binding energy is calculated to 244 kJ/mol.

Upon coordination of NO to FeP in *trans* position to the Ag surface, the Fe−Ag_{top} distance is significantly increased by 0.72 Å to 3.60 Å (PBE+vdW level, i.e., including dispersion), and the binding energy is reduced to 229 kJ/mol. The calculated binding energy without taking into account van der Waals dispersion is

dx.doi.org/10.1021/ja1093502 |J. Am. Chem. Soc. 2011, 133, 6206–6222

Table 2. Calculated NO Binding Energies to Free and Adsorbed MP (M = Co, Fe) in Axial Position[a]

system	kJ/mol (eV)	system	kJ/mol (eV)
CoP	159 (1.65)	CoP−Ag(111)	124 (1.29)
FeP	180 (1.86)	FeP−Ag(111)	168 (1.75)

[a] Energies in kJ/mol and eV; PBE Density-Functional Level.

computed to 15 kJ/mol at the PBE level. These data indicate the absence of any covalent or coordinative bond between the NO-coordinated iron center and the Ag surface. Hence, just as for the CoP/Ag(111) system, our DFT calculations indicate a strong *trans* effect of NO, which essentially turns the chemisorbed FeP molecule into a ON-FeP complex which is merely physisorbed.

Finally, the experimental data reported above suggest that ZnTPP essentially does not interact electronically with the Ag surface. This is confirmed by our density-functional calculations for the ZnP/Ag(111) system. The computed Zn−Ag_{top} distance is calculated to 3.30 Å at the PBE+vdW level, and is thus markedly greater than the corresponding M−Ag_{top} distances for CoP and FeP.

In summary, our periodic DFT calculations suggest that CoP interacts more strongly with a Ag(111) surface than FeP, and that the M−Ag_{top} bonds in both systems are significantly weakened upon NO coordination to MP. The experimental data reported above in Sections 3.1 and 3.2 suggest that NO coordination is reversible at elevated temperatures (500 or 600 K, see above), and that a removal of the NO ligand requires higher temperature for ON−FeTPP/Ag(111) than for ON−CoTPP/Ag(111). It is therefore interesting to consider the energies associated with the coordination (or dissociation) of the NO ligand to (from) these systems. The calculated binding energies of NO to MP are collected in Table 2 for both the gas-phase and the adsorbed MP molecules.

The data suggest that NO binds stronger to FeP by 21 kJ/mol than to CoP in the gas phase. For the adsorbed complexes, the Fe−NO bond is even more favored: The NO detachment from FeP−Ag(111) is less favorable by 44 kJ/mol than from CoP−Ag(111). In general, NO is found to detach more readily from the surface-bound complexes as compared to the free metalloporphyrins. This is because the loss in total bond order, caused by the release of NO, is in part compensated for by the reestablished MP−Ag(111) surface coordinative bond, which is stronger for CoP than for FeP (bond order conservation[89]). This result is in line with our experimental observations reported above, which show that NO desorption from FeTPP monolayers requires higher temperatures than for CoTPP monolayers. The calculated Co−NO and Fe−NO binding energies of 124 and 168 kJ/mol correspond to NO desorption temperatures of 460 and 615 K, respectively, according to an estimate based on the Redhead equation[90] with an assumed frequency factor of 10^{13} s^{-1} and a heating rate of 1 K/s. This is in good agreement with the experimental findings.

According to a partial charge analysis,[70] the entire MP moiety gains 0.37 (M = Co) or 0.22 (M = Fe) electron charges upon interaction with Ag(111). The charge-transfer from the surface to the complex is mitigated for the NO-coordinated complexes, for example, (NO)CoP has a negative charge of only −0.03 e in the presence of the surface. In the isolated complexes (NO)MP (M = Co, Fe), that is, in the absence of the surface, the coordinated NO ligand adopts a negative partial charge of 0.20e for M = Co and 0.35e for M = Fe. (For more details and comparison with the other model systems, see the SI.) Charge transfer from a metal surface to metal complexes has been observed previously for other surface-confined coordination compounds.[91]

In conclusion, the higher NO binding energy to surface-bound Fe(TP)P compared to surface-bound Co(TP)P is thus due to both the higher intrinsic binding energy of NO to Fe(TP)P on one hand and due to the weaker surface coordinative bond on the other hand.

4.3. Interaction of MTPP and (ON)MTPP with a Ag atom. The experimental data and periodic DFT calculations reported so far support the view that coordinated NO exerts a pronounced structural *trans* effect on adsorbed CoP and FeP. The phenomenon of a *trans* effect, however, has its historical roots in molecular coordination chemistry. It is therefore interesting to investigate the *trans* effect of an NO ligand on a single Ag ligand in *trans* position to CoTPP and FeTPP. These coordination compounds incorporating metal−metal bonds represent our second type of model systems. They allow us to better quantify the *trans* effect in terms of the changes in M−Ag distances (M = Co, Fe) induced by the *trans*-coordination of NO in comparison to conventional ligands, and provide a simple and transparent picture of the M−Ag bonding interaction from a molecular orbital (MO) interaction perspective. Moreover, we will now consider the full MTPP molecules instead of the MP models used in our periodic DFT studies. It has been shown before[27,48] that the peripheral phenyl rings can be of relevance in cases where the conformation of the porphyrins is important.

Nevertheless, one might wonder whether coordination of a simple Ag atom bears any resemblance to the surface coordination problem discussed so far. The computed core-level shifts, which agree qualitatively with experimental data, suggest that this is indeed the case (see the SI, Table S2). Moreover, the coordinated Ag atom might be considered, to some approximation, as a representation of the top-site Ag atom of the (111) surface which is closest to the metal centers of the adsorbed metalloporphyrins. Note that a related computational approach was successfully employed to explain the unusual 3-fold coordination of carbonitrile ligands to Co centers identified at the same substrate.[92]

Graphical representations of the optimized molecular geometries (computed at the BP/TZVP level) of *molecular* Ag−MTPP model complexes with and without NO are shown in Figure 11. Structural data of their optimized ground state geometries are listed in Table 3. (See also refs 71 and 93−99 for previous results on NO porphyrin complexes *without* a Ag atom in *trans* position.) Table 4 collects the computed binding energies for various ligand spheres according to the reactions given in Figure 9.

Coordination of NO to MTPP. The binding energy of NO to bare CoTPP is computed to 142 kJ/mol (cf. Table 4, BP/TZVP level, see Section 2.3); this is reasonably close to but somewhat lower than the binding energy to CoP obtained from our periodic DFT calculations reported above (159 kJ/mol, PBE functional). The lowest-energy structure found for (NO)CoTPP features a twisted conformation of the porphyrin core which, leaving the NO ligand aside, can be assigned a S_4 point group symmetry. The ground state of the complex is computed to be a spin singlet, in agreement with the XPS data for (NO)CoTPP multilayers. The ground state of (NO)FeTPP is found to be a spin doublet (cf. also ref.[71]). The ON−Fe bond in (NO)FeTPP (172 kJ/mol; cf.

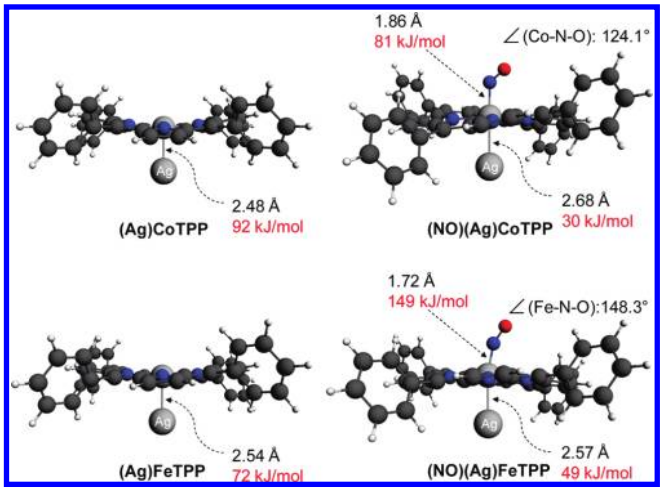

Figure 11. Optimized geometries and ligand binding energies of (Ag)CoTPP (top, left), (NO)(Ag)CoTPP (top, right), (Ag)FeTPP (left, bottom) and (NO)(Ag)FeTPP (right, bottom); BP/TZVP level of theory.

180 kJ/mol for the periodic calculations on NO−FeP) is stronger (by 29 kJ/mol) and shorter (by 0.11 Å) than the corresponding bond in (NO)CoTPP. (NO)FeTPP shows a twisted porphyrin core with the Fe center displaced toward the NO ligand with respect to an imaginary plane defined by the four porphyrin N atoms.

Both the (NO)CoTPP and (NO)FeTPP complexes feature a bent NO ligand. This indicates an NO^- character of the ligand[38] and is thus in agreement with the experimental results, which show a transfer of electron density from the metal center to the NO ligand. (The NO ligand bears a negative partial charge of 0.20e in (NO)CoP or 0.35e in (NO)FeP, see the SI for details.) The angle Fe−N−O of 145° is less acute compared to that found in (NO)CoTPP (123°). This together with the shorter Fe−N(O) distance indicates an increased π-donation from NO to the more electron-deficient Fe center.[95] The Fe−N(O) unit shows a peculiar tilt of the NO ligand toward one side of the TPP core (angles (O)N−Fe−N(por) 87°/94°/102°/103°), an effect which recently has been observed experimentally[100] and explained theoretically.[95]

From the experimental procedure discussed above, we cannot exclude the coordination of *two* NO ligands to MTPP. Additional DFT calculations for $(NO)_2$MTPP show, however, that the binding energy of a second NO ligand in *trans* position to the first NO is rather low (24 kJ/mol for M = Co, 47 kJ/mol for M = Fe). According to the Redhead equation,[90] bond energies of 24 and 47 kJ/mol correspond to desorption temperatures below 100 and 200 K, respectively (assuming a frequency factor of 10^{13} s^{-1}), which means that the second NO ligand should not be bound under the conditions of our experiment.

Coordination of Ag to MTPP. Next, the interaction of the single Ag atom with MTPP (M = Co, Fe) is considered. (Ag)CoTPP in its lowest-energy conformation (spin-singlet ground state) shows a saddle-shaped porphyrin core (close to D_{2d} symmetry) with the usual twist of the peripheral phenyl rings (67°), see Figure 11. The Ag atom is bound to the Co center at a distance of 2.48 Å (cf. Table 3) and with a binding energy of 92 kJ/mol (Table 4, BP/TZVP level). In comparison, for (Ag)FeTPP (doublet ground state, spin contamination S^2 = 1.074), a modest symmetry breaking of the porphyrin core toward a twisted conformation (approximate S_4 symmetry)

Table 3. Salient Geometric Parameters (in angstroms and degrees) from Optimized Geometries of Various MTPP Complexes (M = Co, Fe, Zn)[a]

complex	d(M−NO)	d(M−Ag)	d(N−O)	∠(M−N−O)
(Ag)CoTPP		2.48		
(ON)CoTPP	1.82		1.18	123°
(ON)(Ag)CoTPP	1.86	2.68	1.18	124°
(Ag)FeTPP		2.54		
(ON)FeTPP	1.71		1.18	145°
(ON)(Ag)FeTPP	1.72	2.57	1.18	148°
(Ag)ZnTPP		2.77		

[a] BP/TZVP Level of Theory.

Table 4. Computed NO and Ag Binding Energies (in kJ/mol) in Various MTPP Complexes[a]

complex	NO	Ag
(NO)(Ag)CoTPP	81	30
(NO)(Ag)FeTPP	149	49
(NO)CoTPP	142	
(NO)FeTPP	172	
(Ag)CoTPP		92
(Ag)FeTPP		72
(Ag)ZnTPP		18

[a] BP/TZVP level of theory.

occurs upon coordination of Ag. The Fe−Ag bond is slightly longer (by 0.07 Å) and weaker (by 20 kJ/mol) than the Co−Ag bond (Table 4). In general, all Ag−MTPP bonds are weaker than the corresponding NO−MTPP bonds. In contrast, coordination of a Ag atom to ZnTPP yields a fairly long Zn−Ag distance of 2.77 Å and a very low binding energy of only 18 kJ/mol (see Table 4). This underlines the weakness of the Zn−Ag interaction as suggested by the photoemission data reported above.

For the molecular complexes, the same trends in M−Ag binding energy and bond distances have been found as for the periodic systems above. In particular, the binding energy of the Ag atom or the Ag(111) surface to metalloporphyrins decreases in the order Co(TP)P > Fe(TP)P > Zn(TP)P. However, (leaving van der Waals dispersion corrections aside) the absolute binding energies to a single Ag atom are higher by about 50 kJ/mol than to a Ag(111) surface, and the M−Ag bond lengths in the (Ag)MTPP complexes are shorter than in the surface model (shortest distance M−Ag = 2.48 Å vs 2.88 Å for M = Co, and 2.54 Å vs 3.13 Å for M = Fe). These differences meet our expectations because the single Ag atom is more reactive than a Ag atom with nine nearest Ag neighbors in a Ag(111) surface.

trans-Coordination of NO and Ag to MTPP. The structural data obtained from the periodic DFT calculations suggest that the adsorbed (ON)MP complexes are not covalently bound to the Ag surface for both M = Co, Fe (physisorption), in contrast the MP adsorbates without NO. To further clarify how this *trans* effect[35−39] analogon affects the chemical bond to Ag, we now consider the simultaneous coordination of NO and Ag to CoTPP and FeTPP in the molecular model complexes (NO)(Ag)MTPP (see Figure 11 and the SI).

The computed geometric parameters of the *trans*-(NO)-(Ag)MTPP complexes are collected in Table 3 and Figure 11.

dx.doi.org/10.1021/ja1093502 |*J. Am. Chem. Soc.* 2011, 133, 6206–6222

The Co−Ag distance in (NO)(Ag)CoTPP (spin-doublet ground state) is increased from 2.48 to 2.68 Å upon coordination of the NO ligand, indicating again a pronounced *trans* influence of NO on the Ag−Co bond. The binding energy of the Ag atom is reduced from 92 kJ/mol in (Ag)CoTPP to only 30 kJ/mol. Additional calculations included in the SI (Table S7) show that the structural *trans* effect exerted by NO on Ag is in fact stronger than the one exerted on other ligands such as NH_3, CO, Cl^-, and NCS^-. On the other hand, the local coordination geometry of the NO ligand does not change much upon Ag bonding compared to (NO)CoTPP (Co−N−O angle: 124.2°). We furthermore note that the porphyrin core shows a pronounced twist (ruffling) of the pyrrole rings.

The situation is again somewhat different for (NO)(Ag)FeTPP, in which the Fe−Ag distance (2.57 Å) is only marginally longer than in (Ag)FeTPP (2.54 Å). The dissociation energy of the Ag atom (49 kJ/mol) is reduced by 23 kJ/mol compared to that of (Ag)FeTPP (72 kJ/mol, Table 4). (NO)(Ag)FeTPP is predicted to be a spin singlet, and, like the Co complex, shows a small deviation of the porphyrin core from planarity (approximate S_4 symmetry) with a slight displacement of the Fe center toward the NO ligand. The Fe−N−O angle is similar (148°) as that in (NO)FeTPP (145°), and is thus less acute than in (NO)CoTPP (123°). This agrees well with expectations from the Enemark-Feltham electron count.[101] The Ag−Fe−N(O) unit is not linear but shows an angle of 166° in the optimized geometry (cf. the corresponding angle of 179° in (NO)(Ag)CoTPP). This again reflects the peculiar tilt of the NO ligand toward one side of the TPP core (angles (O)N−Fe−N(por) 88°/89°/103°/103°) which is also observed in (NO)FeTPP.[95,100] All in all, our calculations suggest that Ag and NO ligands do not significantly affect their mutual coordination geometry in FeTPP, unlike the situation for CoTPP.

Electronic Structure. The relevant features of the electronic structure of MTPP (M = Co, Fe) are briefly discussed as a prequel to the analysis of the interaction with Ag and NO. For convenience, the molecular orbitals will be labeled according to the D_{4h} (CoTPP) or D_{2h} (FeTPP) point groups, even if the underlying geometry does not have the full symmetry indicated by these point groups. Furthermore, only those frontier orbitals with significant coefficients for the d-type atomic orbitals of the transition metal center M (i.e., Co or Fe) will be discussed, because these are responsible for the binding of the axial ligands (Ag and NO) to MTPP.

According to the present calculations on the doublet ground state of CoTPP, the degenerate set of Co d_{xz}, d_{yz} atomic orbitals (AOs) labeled $12e_g$ represent the (global) HOMO in the minority spin channel β (at −4.68 eV; majority (α) component is HOMO-4 at −5.07 eV). The d_{z2} AO $25a_{1\,g}$ is singly occupied in CoTPP. This orbital is the LUMO in the β spin channel (−3.76 eV), while the corresponding α spin component is found at lower energy (HOMO-10, −6.26 eV). The d_{x2-y2} spin orbitals are both unoccupied. The remaining d orbitals dominantly participate in occupied MOs and are found within a similar energy range (see the SI for details). In contrast to CoTPP, the d_{z^2} AO (labeled $36a_g$) of the Fe center in the triplet ground state of FeTPP is doubly occupied, the β component being the HOMO (−3.89 eV) while the α component is the HOMO-2 (−4.48 eV). The d_{xz}/d_{yz} AOs ($12b_{2g}$, $12b_{3g}$) are half-occupied, the α spin component being occupied (−5.11 eV), while the β components represent the LUMO and LUMO+1 (−3.30 eV). Further below, these sets of orbitals are shown to be responsible for the binding of the NO or Ag ligands to MTPP. (Detailed listings of computed orbital energies can be found in the SI).

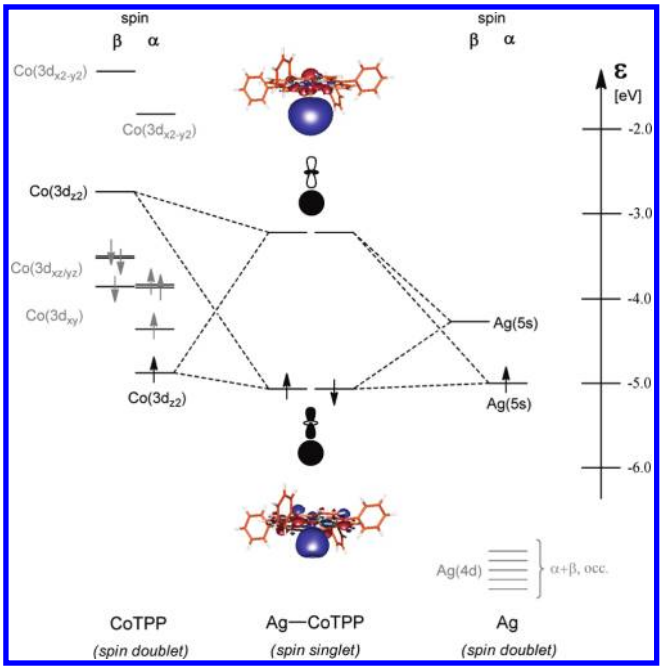

Figure 12. Qualitative orbital energy interaction diagram for the interaction of Ag and CoTPP in the complex (Ag)CoTPP and illustrations of the bonding and antibonding MOs; orbital energies of the CoTPP and Ag fragments have been shifted for illustration purposes; Co and Ag d levels which are not involved in the bonding are shaded. For the (Ag)CoTPP complex, levels not directly involved in the interaction have been omitted for clarity but can be found in the SI.

Electronic Structure of (Ag)MTPP. Figure 12 shows a simplified orbital interaction diagram of the most important contributions to the M−Ag bond in (Ag)MTPP (see Table S6 of the SI for more details). The left-hand side of the Figure shows the orbital energy levels of the CoTPP orbitals (open-shell spin doublet, α is majority spin) with predominant d character, and the right-hand side shows the s-type orbital energy levels of the Ag atom ($4d^{10}5s^1$ electron configuration). The Ag−CoTPP interaction can thus be characterized as a simple two electron, four spin−orbital interaction (or two-electron, two orbital interaction in closed-shell terminology) built by the Ag(5s) (spin) orbital(s) and the M(d_{z2}) (spin) orbital(s). A similar analysis for (Ag)FeTPP leads to an interaction diagram which looks slightly more complicated due to the open-shell character of (Ag)FeTPP but which leads to the same qualitative interpretation, see the SI for details (Figure S5). In summary, the analysis proves a direct, covalent orbital interaction between the metal ion in CoTPP or FeTPP and the Ag ligand, thus giving support for our interpretations of the calculated structural data and the spectroscopic data reported above.

Electronic Structure of (NO)(Ag)MTPP. The electronic structure of (NO)(Ag)MTPP reveals that the covalent part of the Ag−MTPP bond is significantly weakened or virtually disappears if the NO ligand coordinates to the metal center. From previous work on nitrosyl metalloporphyrin complexes,[71,97,101] it is known that the M−NO bond can be decomposed into π- and σ-type interactions mediated by unoccupied π^* orbitals of NO and metal d-orbitals of appropriate local symmetry. On the other hand, we have shown above that the M−Ag interaction in

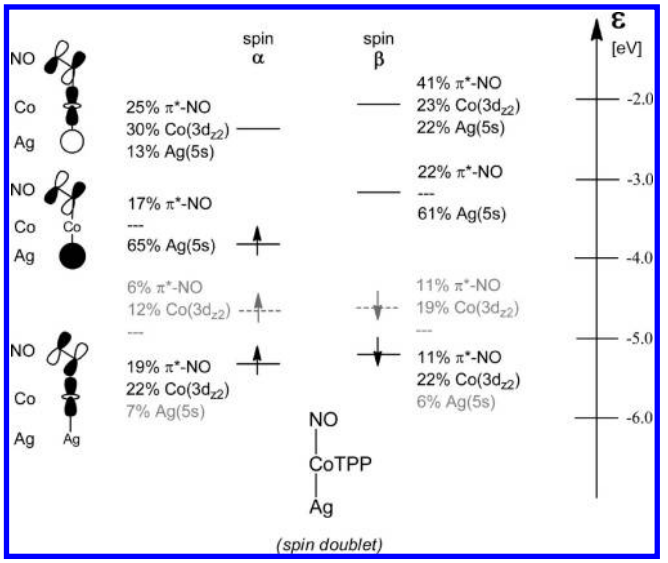

Figure 13. Selected molecular orbitals for the complex (NO)(Ag)CoTPP; orbitals with minor or no Ag(5s) contribution are shaded.

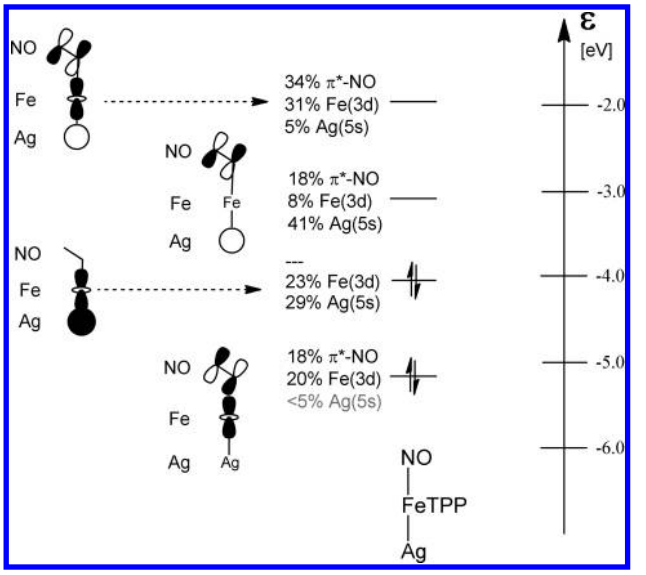

Figure 14. Selected molecular orbitals for the complex (NO)(Ag)FeTPP.

(Ag)MTPP is built by M($3d_{z^2}$) and Ag(5s) orbitals which have local σ-symmetry with respect to the M−Ag axis. To obtain insight into the effect of NO coordination on this bond, we therefore focus our analysis to those molecular orbitals which are (predominantly) composed of these M($3d_{z^2}$) and Ag(5s) orbitals and the π^* orbital of NO which lies in the plane of the ON−M fragment and therefore is capable of forming a σ-bond with the M($3d_{z^2}$) orbital (see Figure 13).

Inspection of the molecular orbitals in (NO)(Ag)CoTPP (some of which are illustrated in Figure 13) shows that almost no direct Co−Ag orbital interaction is discernible in the presence of a *trans*-coordinated NO ligand any more, in contrast to the situation in (Ag)CoTPP. A closer analysis reveals that the lowest (occupied) molecular orbital of the subset shown in Figure 13 represents the σ-type Co−NO interaction and bears only a small contribution (about 7%) of the Ag(5s) orbital, which had been crucial for the covalent Co−Ag bond in (Ag)CoTPP. The main contribution of the Ag(5s) orbital is found in two spin orbitals, one of which is occupied while the other is unoccupied (see Figure 13). However, neither of these orbitals contains a significant contribution from an orbital located on the Co center. In other words, the interaction of the Ag(5s) orbital with the Co($3d_{z^2}$) orbital, which was responsible for the bonding in (Ag)CoTPP, has now essentially vanished, and the Co($3d_{z^2}$) orbital is largely involved in a σ-type interaction with one of the NO π^* orbitals. Please note that the Co−NO bonding mechanism (not shown here) is largely unaffected by the presence of Ag. This observation is in line with the fact that only a fairly small change in the NO−Co bond distance occurs when the Ag binds to (NO)CoTPP (Δd = 0.04 Å, cf. Table 3).

In conclusion, the suppression of the Co−Ag orbital interaction in the presence of an NO ligand can be held responsible for the prolonged Co−Ag distance in (NO)(Ag)CoTPP (Table 3). However, one might argue that such a long distance, howsoever caused, may by itself *prevent* a possible direct orbital interaction between Co and Ag. To exclude this possibility, the NO ligand was deleted from (NO)(Ag)CoTPP *without* relaxing the geometry, that is, a complex (Ag)CoTPP was analyzed where all atoms take those positions at which they are found in the optimized geometry of (NO)(Ag)CoTPP. The main difference to the relaxed structure of (Ag)CoTPP is thus the much longer Ag−Co distance in the unrelaxed structure (Δd = 0.21 Å, cf. Table 3). Inspection of the corresponding (relaxed) MOs shows that, in spite of the long Ag−Co distance, a similar Co(d_{z^2})−Ag(5s) orbital interaction is established (albeit with less mixing, of course; data not shown). This proves that it is indeed the presence of the NO ligand and the resulting competition for the frontier orbitals of Co which weakens the Co(d_{z^2})−Ag(5s) orbital interaction. If, in contrast, the Ag ligand is deleted from (NO)(Ag)CoTPP without relaxing the structure, the orbital interaction pattern describing the bonding of NO to CoTPP is virtually unchanged compared to that of the fully relaxed (NO)CoTPP. This is in line with the above analysis of Co−NO binding in the optimized geometry of (NO)(Ag)CoTPP.

In the iron porphyrin complex (NO)(Ag)FeTPP, the NO induced changes in Fe−Ag bond length are less pronounced, as outlined above. This fact is also reflected by the corresponding orbital interactions, which are sketched in Figure 14. In contrast to the situation with M = Co, the Fe(3d)−Ag(5s) interaction remains partly intact along with the NO−Fe(3d) σ-type interaction, as shown by the doubly occupied molecular orbitals in Figure 14.[103]

4.4. Interaction of CoTPP and (NO)CoTPP with Ag_{19} and Ag_{72} Clusters. The simple (NO)(Ag)MTPP model systems provide an illustrative MO picture of the bonding mechanism and explain the competition between the *trans* ligands, but a single Ag atom cannot represent all properties of a Ag surface. The Ag−M bond in the model systems is likely to be shorter than the actual distance M−Ag(111), due to the increased reactivity of the Ag atom and the neglect of steric repulsions between the TPP framework and the surface. In addition, a single Ag atom is expected to possess a different electron donor capacity as an ensemble of Ag atoms.

To alleviate these limitations and to establish a link between the periodic DFT calculations and the studies on (NO)(Ag)MTPP model systems, another class of model systems

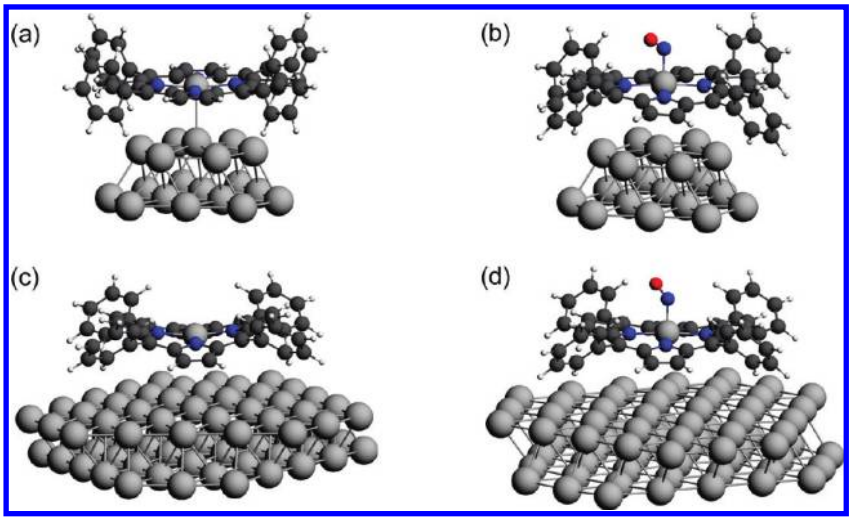

Figure 15. Optimized structures of (a) (Ag_{19})CoTPP, (b) (NO)(Ag_{19})CoTPP, (c) (Ag_{72})CoTPP, (d) (NO)(Ag_{72})CoTPP ; PBE/SV(P) level.

is introduced, in which the Ag(111) surface is approximated by clusters with 19 and 72 Ag atoms. These more complex (and computationally more demanding) model systems may provide a more realistic description of the interaction with a Ag(111) surface but have the drawback that an interpretation of the results is less straightforward than for the (NO)(Ag)MTPP models. We thus restrict ourselves here to a qualitative discussion of the structural changes induced by NO coordination to the (Ag_n)CoTPP (n = 19, 72) model systems, in which the Co ion is located on top of the central Ag atom in the Ag_{19} cluster and above a hollow site in the Ag_{72} cluster, respectively.

Optimized structures of (Ag_n)CoTPP and (NO)(Ag_n)-CoTPP (n = 19, 72) are depicted in Figure 15, and salient structural parameters are collected in Table 5 (see the SI for more details). The computed distance between Co and the nearest Ag atom(s)[104] increases with the cluster size, thus indicating a weaker molecule-cluster interaction for the bigger clusters. For the Ag_{72} cluster, the adsorbed CoTPP molecule undergoes a saddle-shape distortion of the porphyrin core, accompanied by rotation of the peripheral phenyl rings of TPP toward the molecular plane (cf. the SI for details on the geometry.) This can be explained by steric repulsions of these phenyl rings and the Ag surface. Our computational results agree with a combined STM and NEXAFS study of CoTPP on Cu(111), in which the CoTPP molecule was found to acquire a saddle-shaped conformation in the adsorbed state.[105] Similar observations were made for CoTPP on Ag(111).[27,32,33]

Upon NO coordination to the Co center, the Co−Ag distance increases significantly. The relative increase in this distance is larger for the bigger clusters than for the Ag_1 model (+8% for Ag_1, +20% for Ag_{19}, see Table 5, cf. also Table 1). This is probably due to the fact that for the bigger clusters the interaction between Co and Ag becomes weaker in general and is therefore even less capable of competing with the *trans*-coordinated NO, the binding of which to Co is largely unchanged by the Ag cluster. For the biggest cluster model (NO)(Ag_{72})CoTPP, just as for the periodic calculations on Ag(111), the Co center is pulled away from the Ag cluster by the coordinated NO (cf. the SI for details on the computed geometry). These results on finite cluster models confirm again the strong *trans* effect of NO on the interaction of CoTPP with the Ag substrate.

Table 5. Salient Geometric Parameters (in angstroms and degrees) from Optimized Geometries of (Ag_n)CoTPP and (NO)(Ag_n)CoTPP Adsorbate Cluster Models, n = 1, 19, 72[a]

model complex	d(M−N(O))	d(M−Ag)	d(N−O)	∠(M−N−O)
(Ag)CoTPP		2.48		
(Ag_{19})CoTPP		2.80		
(Ag_{72})CoTPP		3.6−3.7		
(ON)(Ag)CoTPP	1.86	2.68	1.18	124°
(ON)(Ag_{19})CoTPP	1.81	3.37	1.17	123°
(ON)(Ag_{72})CoTPP	1.81	>4	1.17	123°

[a] PBE/SV(P) level of theory (correction for van der Waals dispersion not included).

5. DISCUSSION

This study focuses on the question how the chemical bond of a coordinated metal center to a surface is influenced by additional ligands in *trans* position to the surface. Previous theoretical analysis of molecular complexes shows that it is energetically unfavorable for *trans* ligands to share the same orbitals of the central metal ion.[38,106] In general, it was found that σ- and π-bonding effects must be considered for a full mechanistic understanding. In a complex with the *trans*-positioned ligands L_S and L_W, both ligands donate electron density to the metal center M via a σ bond. If L_S is a stronger donor that L_W, then the σ-bond M−L_W will be weakened (L_S→M···L_W). The strong structural *trans* effects of H^- and R^-, which are exclusively σ donor ligands, are attributed to this mechanism (σ *trans* effect). In addition, M can donate electron density from occupied d levels into empty (usually non- or antibonding) ligand orbitals via a π-type interaction. This *back-donation* increases the bond strength of the ligand that is the stronger acceptor at the expense of the M−L bond of the other (weaker) ligand (L_S←M···L_W).[39] In nitrosyl complexes (NO)ML_n, the NO ligand can bind in a linear or a bent geometry. If it adopts a bent bonding mode, as is the case for the systems investigated here (see Section 4), it is a very strong σ donor, but also engages in π-backbonding and is known to exert a particularly strong structural *trans* effect on a wide range of ligands in *trans*-position.[38] An NO-related *trans* effect has previously also been observed on metalloporphyrin-nitrosyl

Table 6. NO Induced Changes of Bond Length, Bond Energy and XPS Co($2p_{3/2}$) Core Level Shifts for the CoTPP System

		(Ag)CoTPP	(NO)(Ag)CoTPP	Δ
d_{Co-Ag} in Å		2.48	2.68	+0.20
E_{Co-Ag} in kJ/mol		92	30	−62
Co($2p_{3/2}$) XPS shifts[a] in eV	exp.	−1.8	−0.4	
	theor.[b]	−0.6	−0.2	

[a] Relative to the CoTPP or (NO)CoTPP *without* the Ag ligand (multilayers of the complexes in the experiment and CoTPP or (NO)CoTPP molecule in the calculation). [b] Slater transition state calculations; cf. Table S2 in the SI for more detail.

complexes, in which the NO ligand influences amino acid ligands coordinated to metalloporphyrins; this effect is very important for biological signaling processes.[71,95]

On a phenomenological level, the concept of the *trans* effect[35−39] has only recently been applied by us to surface chemistry.[30,34] From the point of view of an adsorbed metal complex, the surface which interacts with the metal center can be considered as an unusually bulky ligand with a "cone angle"[107] of 180°. As such, it can influence the electronic properties of the complexed metal ion, as has been shown in Section 3 for Fe and Co porphyrins: The interaction of the coordinated Fe and Co ions with the Ag substrate results in substantial Fe(2p) and Co(2p) core-level shifts and the occurrence of new valence states in the UP and ST spectra, which reveal the covalent character of this interaction. In contrast, no indications for bond formation were found for Zn porphyrin. As shown above, coordination of NO to the Co and Fe centers leads to an almost complete suppression of the electronic interaction with the surface: the core-level shifts are reversed and the new valence states disappear. These observations can be interpreted as manifestations of the *trans* effect with NO as the stronger and Ag as the weaker ligand. The process of formation and cleavage of the substrate-metal bond is fully reversible: if the NO ligands are removed by thermal desorption, the interaction between surface and metal center is restored. Furthermore, in agreement with the expectation of CO ligands showing a weak *trans* effect, recent findings revealed that the surface bonding of CoTPP and FeTPP adsorbed on Ag(111) or Cu(111) is only weakly affected by carbonyl ligation.[108]

Detailed mechanistic insight into the surface *trans* effect is provided by our DFT calculations of the coordination of NO to Co and Fe porphyrins both with and without a Ag atom, a Ag cluster or a Ag(111) surface in *trans* position. The different model systems emphasize complementary aspects of the effect. In particular, the seemingly simplistic model bearing just a single Ag atom provides a direct link to molecular coordination chemistry and allows for a conceptual, qualitative interpretation of the local bonding situation. (Note that coordinative metal−metal bonds between a central transition metal ion and metal-containing ligands are not unusual and occur for example in stannylene complexes,[109] for which also *trans* effects have been reported.[110]) Here, the Ag atom can be envisaged as the simplest approximation of a top-site Ag atom in a real surface. The calculations show that NO binds in the bent mode in all cases and is thus likely to exert a very strong *trans* effect. In agreement with this expectation, the strength of the bond between the Ag atom, cluster, or surface and the transition metal ion (M = Fe, Co) changes dramatically upon NO coordination. (Some illustrative DFT results and experimental data for the (NO)(Ag)CoTPP system are summarized in Table 6.) The magnitude of this *trans* effect also depends on the nature of the complexed metal center M in MTPP.

In line with the NO-induced reduction of the M−Ag bond *energies*, the respective bond *lengths* increase. The periodic calculations of MP on Ag(111) show that the M−Ag_{top} distances are increased upon NO coordination and indicate a physisorption situation. The molecular model complexes, which allow for a more precise quantification of the structural *trans* effect, show that the effect of NO coordination is larger for the Ag−Co (+0.20 Å) than for the Ag−Fe bond (+0.03 Å). These values agree with data for other Co and Fe nitrosyl complexes with bent NO ligands, where the bond length to various *trans* ligands increases between 0.04 and 0.29 Å (see ref 38 and Table S7 of the SI).

The calculations also illustrate the mutual nature of the *trans* effect: While the NO ligand weakens the M−Ag bond, the Ag atom also weakens the M−NO bond, but to a lesser extent, because the Ag atom is the inferior *trans* ligand. For the molecular model complexes, the M−NO binding energy is reduced by −43% for M = Co and −13% for M = Fe upon coordination of the Ag atom.

The frontier orbitals of (Ag)MTPP (Figures 12 and S5) reveal that the Ag−M bond is a covalent two-electron, two-orbital interaction which involves the Ag(5s) and the M(d_{z^2}) orbitals. Upon coordination of NO (Figures 13, 14), this bond is suppressed or weakened, and the Ag(5s) orbitals become largely nonbonding for the case of CoTPP. Instead of interacting with the Ag(5s) orbital, the M(d_{z^2}) orbital engages in a σ-type bond to the NO π_x^* orbital, combined with a π-type interaction between the NO π^* and the Co(d_{xz}/d_{yz}) orbitals. In (NO)(Ag)FeTPP, the Ag(5s) orbital is still involved in the Fe−Ag bond, but to a lesser extent than in the absence of NO.

Additional calculations on finite cluster model systems (Ag_{19} and Ag_{72}) further support our interpretation of the experimental data. For (Ag_{19})CoTPP, a Co−Ag bond length of 2.8 Å is calculated, which is between the lengths of Ag−Ag (2.90 Å) and the Co−Co (2.52 Å) bond and thus in the range of typical covalent or metallic bonds. Upon coordination of NO to the Co ion, the Co−Ag bond length increases by 20% to 3.37 Å, proving substantial weakening of this bond.

The calculations predict that CoTPP interacts more strongly with Ag than FeTPP, while the interaction of NO with FeTPP is stronger than that with CoTPP. This agrees with experimental results, which show that the decomposition temperature of adsorbed (NO)FeTPP is higher than that of adsorbed (NO)CoTPP and that NO coordination to a FeTPP monolayer leads to an larger M(2p) XPS shift than for the CoTPP monolayer (+2.7 vs +2.2 eV).

The validity of our model systems is confirmed by the computed core level shifts (see Table 6 and the SI, Table S2), which are in qualitative agreement with the XPS data. All models predict a reduction in Co(2p) binding energies when CoTPP binds to the Ag atom or Ag(111) surface, in agreement with the experimental XPS shift between multilayer and monolayer. (Expectedly, the calculated shift is smaller, because a single Ag atom has less capacity to influence the Co ion than the Ag(111) surface. This holds both for initial state effects, for example, electron donation, and final state effects, for example, core hole screening.) Most importantly, the experimental finding that NO coordination counteracts the influence of the Ag ligand and leads

to an increase of the Fe(2p) and Co(2p) binding energies is reproduced by the calculations. The computed core level shifts, bond lengths and binding energies thus give support to the interpretation deduced from the XPS experiments, namely, that the interaction of the coordinated metal center with the Ag substrate can be significantly reduced due to the coordination of NO.

6. SUMMARY AND CONCLUSIONS

Adsorption of iron(II) and cobalt(II) tetraphenylporphyrin (FeTPP, CoTPP) on Ag(111) results in the formation of a covalent bond between the coordinated metal center and the Ag surface. For zinc(II) tetraphenylporphyrin (ZnTPP), no bond formation was observed, indicating that the bond strength depends on the electronic structure of the metal center. Coordination of a nitrosyl (NO) ligand to the metal centers of FeTPP and CoTPP leads to a reversible suppression of the bond to the substrate. This was concluded from XPS, UPS and STM/STS experiments and confirmed by DFT calculations on molecular and periodic model systems of the type (NO)(Ag_n)M(TP)P (n = 1, 19, 72, ∞). Specifically, the adsorption of the Co and Fe porphyrins on the Ag substrate leads to new valence states in UPS and STS and to substantial core-level shifts in XPS. DFT reveals that the M−Ag bond can locally be described as a covalent two-orbital, two-electron bond between the Ag(5s) and M($3d_{z^2}$) orbitals. Upon coordination of NO, which adopts a bent geometry, this bonding interaction is suppressed and the Ag(5s) orbitals become nonbonding in CoTPP and weakly bonding in FeTPP. Structural data obtained from the periodic and nonperiodic DFT calculations show that the M−Ag bond length increases upon NO coordination.

For a conceptual understanding of these effects, we have applied principles of chemical bonding in transition metal complexes to the field of surface-confined coordination chemistry.[30,111] In particular, the concept of the *trans effect* proved suitable for the qualitative interpretation of the competition between the bonds of the NO ligand, and silver substrate, to the transition metal centers. The similarity of the results obtained from molecular and periodic model systems emphasizes the close relationship of the classical *trans* effect and the surface *trans* effect, which we have analyzed here in detail. This effect has important implications for the potential catalytic activity or sensor functionality of adsorbed metal complexes. Our results show that the substrate surface can sensitively influence the electronic structure and, thus, the reactivity of the metal centers. The strength of this substrate influence, however, is also controlled by the additional ligands on the metal center, that is, by potential reactant molecules. Depending on the relative strengths of the *trans* influence (the *trans* activity of the ligands), either the substrate or, as is the case for the systems described here, the additional ligand can dominate the electronic properties of the metal center. On the basis of this systematic insight, the interaction between the metal center and the surface can be adjusted with respect to a desired reactivity. This approach mimics, to some extent, enzymatic systems such as heme-thiolate proteins, in which an axial thiolate ligand controls the reactivity of the metal center. Our findings illustrate how the electronic state (including the spin state and thus the magnetic properties) and the reactivity of an adsorbed, complexed metal center results from a delicate interplay between the influences of the surface and the coordinated reactant on this metal center.

■ ASSOCIATED CONTENT

Supporting Information. Additional UP and N(1s) XP spectra, UP signal positions, additional information on the computed structures, electronic structure, and core-level shifts. This material is available free of charge via the Internet at http://pubs.acs.org.

■ AUTHOR INFORMATION

Corresponding Author

Dr. Michael Gottfried, Lehrstuhl für Physikalische Chemie II, Department Chemie and Pharmazie, Universität Erlangen-Nürnberg, Egerlandstr. 3, 91058 Erlangen, Germany. Tel. +49-9131-8527320. Fax +49-9131-8528867. E-mail: michael.gottfried@chemie.uni-erlangen.de. Dr. Wolfgang Hieringer, Theoretische Chemie, Department Chemie and Pharmazie, Universität Erlangen-Nürnberg, Egerlandstr. 3, 91058 Erlangen, Germany. Tel. +49-9131-85-28646. Fax +49-9131-85-27736. E-mail: hieringer@chemie.uni-erlangen.de

■ ACKNOWLEDGMENT

Financial support by the Deutsche Forschungsgemeinschaft through Sonderforschungsbereich 583 and the Cluster of Excellence "Engineering of Advanced Materials" and by the ERC Advanced Grant MolArt (247299) and TUM-IAS is gratefully acknowledged. We thank W. G. Schmidt for sharing with us his van der Waals DFT module for the VASP program.

■ REFERENCES

(1) Hulsken, B.; Van Hameren, R.; Gerritsen, J. W.; Khoury, T.; Thordarson, P.; Crossley, M. J.; Rowan, A. E.; Nolte, R. J. M.; Elemans, J. A. A. W.; Speller, S. *Nat. Nanotechnol.* **2007**, *2*, 285–289.

(2) Mochida, I.; Suetsugu, K.; Fujitsu, H.; Takeshita, K. *J. Phys. Chem.* **1983**, *87*, 1524–1529.

(3) Berner, S.; Biela, S.; Ledung, G.; Gogoll, A.; Backvall, J. E.; Puglia, C.; Oscarsson, S. *J. Catal.* **2006**, *244*, 86–91.

(4) Hassan, S. A.; Hassan, H. A.; Hashem, K. M.; Dayem, H. M. A. *Appl. Catal., A* **2006**, *300*, 14–23.

(5) Ferreira, A. D. Q.; Vinhado, F. S.; Iamamoto, Y. *J. Mol. Catal. A* **2006**, *243*, 111–119.

(6) Mochida, I.; Suetsugu, K.; Fujitsu, H.; Takeshita, K. *J. Catal.* **1982**, *77*, 519–526.

(7) Mochida, I.; Tsuji, K.; Suetsugu, K.; Fujitsui, H.; Takeshita, K. *J. Phys. Chem.* **1980**, *84*, 3159–3162.

(8) Rakow, N. A.; Suslick, K. S. *Nature* **2000**, *406*, 710–713.

(9) Gulino, A.; Gupta, T.; Mineo, P. G.; van der Boom, M. E. *Chem. Commun.* **2007**, 4878–4880.

(10) Takulapalli, B. R.; Laws, G. M.; Liddell, P. A.; Andreasson, J.; Erno, Z.; Gust, D.; Thornton, T. J. *J. Am. Chem. Soc.* **2008**, *130*, 2226–2233.

(11) Andringa, A. M.; Spijkman, M. J.; Smits, E. C. P.; Mathijssen, S. G. J.; van Hal, P. A.; Setayesh, S.; Willard, N. P.; Borshchev, O. V.; Ponomarenko, S. A.; Blom, P. W. M.; de Leeuw, D. M. *Org. Electron.* **2010**, *11*, 895–898.

(12) Di Natale, C.; Monti, D.; Paolesse, R. *Mater. Today* **2010**, *13*, 37–43.

(13) Scudiero, L.; Barlow, D. E.; Mazur, U.; Hipps, K. W. *J. Am. Chem. Soc.* **2001**, *123*, 4073–4080.

(14) Hipps, K. W.; Scudiero, L.; Barlow, D. E.; Cooke, M. P. *J. Am. Chem. Soc.* **2002**, *124*, 2126.

(15) Barlow, D. E.; Scudiero, L.; Hipps, K. W. *Langmuir* **2004**, *20*, 4413–4421.

(16) Katsonis, N.; Vicario, J.; Kudernac, T.; Visser, J.; Pollard, M. M.; Feringa, B. L. *J. Am. Chem. Soc.* **2006**, *128*, 15537–15541.
(17) Auwärter, W.; Weber-Bargioni, A.; Riemann, A.; Schiffrin, A.; Gröning, O.; Fasel, R.; Barth, J. V. *J. Chem. Phys.* **2006**, *124*, 194708.
(18) Buchner, F.; Comanici, K.; Jux, N.; Steinrück, H.-P.; Marbach, H. *J. Phys. Chem. C* **2007**, *111*, 13531–13538.
(19) Buchner, F.; Schwald, V.; Comanici, K.; Steinrück, H.-P.; Marbach, H. *ChemPhysChem* **2007**, *8*, 241–243.
(20) Buchner, F.; Flechtner, K.; Bai, Y.; Zillner, E.; Kellner, I.; Steinrück, H.-P.; Marbach, H.; Gottfried, J. M. *J. Phys. Chem. C* **2008**, *112*, 15458–15465.
(21) Sekiguchi, T.; Wakayama, Y.; Yokoyama, S.; Kamikado, T.; Mashiko, S. *Thin Solid Films* **2004**, *464*−*65*, 393–397.
(22) Nilson, K.; Åhlund, J.; Brena, B.; Göthelid, E.; Schiessling, J.; Mårtensson, N.; Puglia, C. *J. Chem. Phys.* **2007**, *127*, 114702.
(23) Åhlund, J.; Schnadt, J.; Nilson, K.; Göthelid, E.; Schiessling, J.; Besenbacher, F.; Mårtensson, N.; Puglia, C. *Surf. Sci.* **2007**, *601*, 3661–3667.
(24) Cheng, Z. H.; Gao, L.; Deng, Z. T.; Jiang, N.; Liu, Q.; Shi, D. X.; Du, S. X.; Guo, H. M.; Gao, H.-J. *J. Phys. Chem. C* **2007**, *111*, 9240–9244.
(25) Walzer, K.; Hietschold, M. *Surf. Sci.* **2001**, *471*, 1–10.
(26) Gopakumar, T. G.; Lackinger, M.; Hackert, M.; Müller, F.; Hietschold, M. *J. Phys. Chem. B* **2004**, *108*, 7839–7843.
(27) (a) Buchner, F.; Warnick, K.-G.; Wölfle, T.; Görling, A.; Steinrück, H.-P.; Hieringer, W.; Marbach, H. *J. Phys. Chem. C* **2009**, *113*, 16450–16457. (b) Seufert, K.; Auwärter, W.; Barth, J. V. *J. Am. Chem. Soc.* **2010**, *132*, 18141–18146.
(28) Buchner, F.; Kellner, I.; Hieringer, W.; Görling, A.; Steinrück, H.-P.; Marbach, H. *Phys. Chem. Chem. Phys.* **2010**, *12*, 13082.
(29) Auclair, K.; Moenne-Loccoz, P.; Ortiz de Montellano, P. R. *J. Am. Chem. Soc.* **2001**, *123*, 4877–4885.
(30) Gottfried, J. M.; Marbach, H. *Z. Phys. Chemie* **2009**, *223*, 53–74.
(31) Lukasczyk, T.; Flechtner, K.; Merte, L. R.; Jux, N.; Maier, F.; Gottfried, J. M.; Steinrück, H. P. *J. Phys. Chem. C* **2007**, *111*, 3090–3098.
(32) Bai, Y.; Buchner, F.; Kellner, I.; Schmid, M.; Vollnhals, F.; Steinrück, H.-P.; Marbach, H.; Gottfried, J. M. *New J. Phys.* **2009**, *11*, 125004.
(33) Auwärter, W; Seufert, K; Klappenberger, F.; Reichert, J.; Weber-Bargioni, A.; Verdini, A.; Cvetko, D.; Dell'Angela, M.; Floreano, L.; Cossaro, A.; Bavdek, A.; Morgante, A.; Seitsonen, A. P.; Barth, J. V. *Phys. Rev. B* **2010**, *81*, 245403.
(34) Flechtner, K.; Kretschmann, A.; Steinrück, H.-P.; Gottfried, J. M. *J. Am. Chem. Soc.* **2007**, *129*, 12110–12111.
(35) Appleton, T. G.; Clark, H. C.; Manzer, L. E. *Coord. Chem. Rev.* **1973**, *10*, 335–422.
(36) Hartley, F. R. *Chem. Soc. Rev.* **1973**, *2*, 163–179.
(37) Atwood, J. D. *Inorganic and Organometallic Reaction Mechanisms*, 2nd ed.; VCH: Weinheim, 1997.
(38) Coe, B. J.; Glenwright, S. J. *Coord. Chem. Rev.* **2000**, *203*, 5–80.
(39) Jordan, R. B. *Reaction Mechanisms of Inorganic and Organometallic Systems*, 3rd ed.; Oxford University Press Inc: New York, 2007.
(40) Wackerlin, C.; Chylarecka, D.; Kleibert, A.; Müller, K.; Iacovita, C.; Nolting, F.; Jung, T. A.; Ballav, N. *Nat. Commun.* **2010**, *1*, 61.
(41) Suarez, S. A.; Fonticelli, M. H.; Rubert, A. A.; de la Llave, E.; Scherlis, D.; Salvarezza, R. C.; Marti, M. A.; Doctorovich, F. *Inorg. Chem.* **2010**, *49*, 6955–6966.
(42) Domke, K. F.; Pettinger, B. *Chemphyschem* **2009**, *10*, 1794–1798.
(43) Isvoranu, C.; Wang, B.; Schulte, K.; Ataman, E.; Knudsen, J.; Andersen, J. N.; Bocquet, M. L.; Schnadt, J. *J. Phys.-Condens. Matter* **2010**, *22*, 472002.
(44) Kretschmann, A.; Walz, M.-M.; Flechtner, K.; Steinrück, H.-P.; Gottfried, J. M. *Chem. Commun.* **2007**, 568–570.
(45) Gottfried, J. M.; Flechtner, K.; Kretschmann, A.; Lukasczyk, T.; Steinrück, H. P. *J. Am. Chem. Soc.* **2006**, *128*, 5644–5645.
(46) Shubina, T. E.; Marbach, H.; Flechtner, K.; Kretschmann, A.; Jux, N.; Buchner, F.; Steinrück, H.-P.; Clark, T.; Gottfried, J. M. *J. Am. Chem. Soc.* **2007**, *129*, 9476–9483.
(47) Auwärter, W.; Weber-Bargioni, A.; Brink, S.; Riemann, A.; Schiffrin, A.; Ruben, M.; Barth, J. V. *ChemPhysChem* **2007**, *8*, 250–254.
(48) Buchner, F.; Seufert, K.; Auwärter, W.; Heim, D.; Barth, J. V.; Flechtner, K.; Gottfried, J. M.; Steinrück, H.-P.; Marbach, H. *ACS Nano* **2009**, *3*, 1789–1794.
(49) Auwärter, W.; Schiffrin, A.; Weber-Bargioni, A.; Pennec, Y.; Riemann, A.; Barth, J. V. *Int. J. Nanotechnol.* **2008**, *5*, 1171–1193.
(50) www.createc.de.
(51) Parr, R. G.; Yang, W. *Density-Functional Theory of Atoms and Molecules*; Oxford University Press: New York, 1989.
(52) Koch, W.; Holthausen, M. C. *A Chemist's Guide to Density Functional Theory*, 1st ed.; Wiley-VCH: Weinheim, 2000.
(53) Kresse, G; Hafner, J. *Vienna Ab Initio Simulation Package (VASP)*, version 4.6; Institut für Materialphysik, Universität Wien: Vienna, since 1991; www.vasp.at.
(54) Ahlrichs, R.; et al. *Turbomole*, version 5.7; University of Karlsruhe: Karlsruhe, since 1988; www.turbomole.com.
(55) Baerends, E. J.; et al. *Amsterdam Density-Functional Package (ADF)*, version 2007, Vrije Universiteit Amsterdam, Amsterdam, since 1978; www.scm.com.
(56) Perdew, J. P.; Burke, K.; Ernzerhoff, M. *Phys. Rev. Lett.* **1996**, *77*, 3865.
(57) Blöchl, P. E. *Phys. Rev. B* **1994**, *50*, 17953.
(58) Kresse, G.; Joubert, D. *Phys. Rev. B* **1999**, *59*, 1758.
(59) Ortmann, F.; Bechstedt, F.; Schmidt, W. G. *Phys. Rev. B* **2006**, *73*, 205101.
(60) Becke, A. D. *Phys. Rev. A* **1988**, *38*, 3098.
(61) Perdew, J. P. *Phys. Rev. B* **1986**, *33*, 8822.
(62) Weigend, F.; Ahlrichs, R. *Phys. Chem. Chem. Phys.* **2005**, *7*, 3297–3305.
(63) Eichkorn, K.; Treutler, O.; Öhm, H.; Häser, M.; Ahlrichs, R. *Chem. Phys. Lett.* **1995**, *240*, 283–290.
(64) Sierka, M.; Hogekamp, A.; Ahlrichs, R. *J. Chem. Phys.* **2003**, *118*, 9136.
(65) te Velde, G.; Bickelhaupt, F. M.; Baerends, E. J.; Fonseca Guerra, C.; van Gisbergen, S. J. A.; Snijders, J. G.; Ziegler, T. *J. Comput. Chem.* **2001**, *22*, 931–967.
(66) Slater, J. C. *Adv. Quantum Chem.* **1972**, *6*, 1–92.
(67) Birgersson, M.; Almbladh, C.-O.; Borg, M.; Andersen, J. N. *Phys. Rev. B* **2003**, *67*, 045402.
(68) Egelhoff, W. F. *Surf. Sci. Rep* **1987**, *6*, 253–415.
(69) Johansson, B.; Martensson, N. *Phys. Rev. B* **1980**, *21*, 4427.
(70) (a) Bader, R. F. W. *Atoms in Molecules: A Quantum Theory*; Oxford University Press: New York, 1990. (b) Tang, W.; Sanville, E.; Henkelman, G. *J. Phys.: Condens. Matter* **2009**, *21*, 084204.(c) The *bader* program by Arnaldsson, A.; Tang, W.; , Henkelman, G.; , version 0.27a, has been used to perform the partial charge analysis; http://theory.cm.utexas.edu/vtsttools/bader.
(71) Ghosh, A. *Acc. Chem. Res.* **2005**, *38*, 943–954.
(72) Ghosh, A. In *The Porphyrin Handbook*; Kadish, K. M., Smith, K. M., Guilard, R., Eds.; Academic Press: San Diego, CA, 2000; Vol. 7, p 1−38.
(73) Collman, J. P.; Hoard, J. L.; Kim, N.; Lang, G.; Reed, C. A. *J. Am. Chem. Soc.* **1975**, *97*, 2676–2681.
(74) Due to a spin equilibrium, fractions of the Fe ions may exist in a singlet state (cf. Lecomte, C.; Rohmer, M.-M.; Benard, M. In *The Porphyrin Handbook*; Kadish, K. M., Smith, K. M., Guilard, R., Eds.; Academic Press: San Diego, 2000; Vol. 7, p 39; Scheidt, W. R. In *The Porphyrin Handbook*; Kadish, K. M., Smith, K. M., Guilard, R., Eds.; Academic Press: San Diego, 2000; Vol. 3, p 49; Collman, J. P.; Hoard, J. L.; Kim, N.; Lang, G.; Reed, C. A. *J. Am. Chem. Soc.* **1975**, *97*, 2676–2681) or a quintet state, cf. ref 46.
(75) Grosvenor, A. P.; K., B. A; Biesinger, M. C.; McIntyre, N. S. *Surf. Interface Anal.* **2004**, *36*, 1564–1574.
(76) Sanders, J. K. M.; Bampos, N.; Clyde-Watson, Z.; Darling, S. L.; Hawley, J. C.; Kim, H.-J.; Mak, C. C.; Webb, S. J. In *The Porphyrin Handbook*; Kadish, K. M., Smith, K. M., Guilard, R., Eds.; Academic Press: San Diego, 2000; Vol. 3, pp 1−48.

(77) Bai, Y.; Buchner, F.; Wendahl, M. T.; Kellner, I.; Bayer, A.; Steinrück, H.-P.; Marbach, H.; Gottfried, J. M. *J. Phys. Chem. C* **2008**, *112*, 6087–6092.
(78) Note that the distance between the Fe ion and the Ag surface may be different for FePc and FeTPP, because the peripheral phenyl groups of FeTPP act as spacer groups, cf. ref 31. This would also influence the magnitude of the ion-surface interaction.
(79) Flechtner, K.; Kretschmann, A.; Bradshaw, L. R.; Walz, M. M.; Steinrück, H. P.; Gottfried, J. M. *J. Phys. Chem. C* **2007**, *111*, 5821–5824.
(80) Liao, M.-S.; Scheiner, S. *J. Chem. Phys.* **2002**, *117*, 205–219.
(81) Comanici, K.; Buchner, F.; Flechtner, K.; Lukasczyk, T.; Gottfried, J. M.; Steinrück, H. P.; Marbach, H. *Langmuir* **2008**, *24*, 1897–1901.
(82) Zotti, L. A.; Teobaldi, G.; Hofer, W. A.; Auwärter, W.; Weber-Bargioni, A.; Barth, J. V. *Surf. Sci.* **2007**, *601*, 2409–2414.
(83) Rovira, C.; Kunc, K.; Hutter, J.; Ballonelt, P.; Parrinello, M. *J. Phys. Chem. A* **1997**, *101*, 8914–8925.
(84) Liao, M.-S.; Scheiner, S. *J. Chem. Phys.* **2001**, *114*, 9780–9791.
(85) Nguyen, K. A.; Pachter, R. *J. Chem. Phys.* **2001**, *114*, 10757–10767.
(86) Vangberg, T.; Ghosh, A. *J. Am. Chem. Soc.* **1999**, *121*, 12154–12160.
(87) Wölfle, T.; Görling, A.; Hieringer, W. *Phys. Chem. Chem. Phys.* **2008**, *10*, 5739.
(88) Cordero, B.; Gómez, V.; Platero-Prats, A. E.; Revés, M.; Echeverría, J.; Cremades, E.; Barragán, F.; Alvarez, S. *Dalton Trans.* **2008**, 2832–2838.
(89) Shustorovich, E. *Surf. Sci. Rep.* **1986**, *6*, 1–63.
(90) Redhead, P. A. *Vacuum* **1962**, *12*, 203–211.
(91) Shi, X. Q.; Lin, C.; Minot, C.; Tseng, T.-C.; Tait, S. L.; Lin, N.; Zhang, R. Q.; Kern, K.; Cerdá, J. I.; Van Hove, M. A. *J. Phys. Chem. C* **2010**, *114*, 17197–17204.
(92) Schlickum, U.; Decker, R.; Klappenberger, F.; Zoppellaro, G.; Klyatskaya, S.; Ruben, M.; Silanes, I.; Arnau, A.; Kern, K.; Brune, H.; Barth, J. V. *Nano Lett.* **2007**, *7*, 3813–3817.
(93) Nappa, M.; Valentine, J. S. *J. Am. Chem. Soc.* **1978**, *100*, 5075–5080.
(94) Groves, J. T.; Roman, J. S. *J. Am. Chem. Soc.* **1995**, *117*, 5594–95.
(95) Ghosh, A.; Wondimagegn, T. *J. Am. Chem. Soc.* **2000**, *122*, 8101–8102.
(96) Selcuki, C.; van Eldik, R.; Clark, T. *Inorg. Chem.* **2004**, *43*, 2828–2833.
(97) Praneeth, V. K. K.; Neese, F.; Lehnert, N. *Inorg. Chem.* **2005**, *44*, 2570–2572.
(98) Lehnert, N.; Praneeth, V. K. K.; Paulat, F. *J. Comput. Chem.* **2006**, *27*, 1338–1351.
(99) Nakashima, H.; Hasegawa, J.-Y.; Nakatsuji, H. *J. Comput. Chem.* **2006**, *27*, 426–433.
(100) Scheidt, W. R.; Ellison, M. K. *Acc. Chem. Res.* **1999**, *32*, 350–359.
(101) Enemark, J. H.; Feltham, R. D. *Coord. Chem. Rev.* **1974**, *13*, 339–406.
(102) Paulat, F.; Lehnert, N. *Inorg. Chem.* **2007**, *46*, 1547–1549.
(103) It appears to the alert reader that we construct four molecular orbitals from only three fragment orbitals here. Please note, however, that other fragments orbitals (e.g., from the porphyrin ligand) also mix in to these orbitals but are not shown for simplicity. The orbitals we show here are those which bear a major contribution from the relevant fragment orbitals which are included in the analysis.
(104) For the hollow-site coordination of CoTPP to the Ag_{72} cluster, the distance discussed corresponds to the distance between the Co atom and the plane defined by the three adjacent Ag atoms confining the hollow site.
(105) Weber-Bargioni, A.; Auwärter, W.; Klappenberger, F.; Reichert, J.; Lefrancois, S.; Strunskus, T.; Wöll, C.; Schiffrin, A.; Pennec, Y.; Barth, J. V. *ChemPhysChem* **2008**, *9*, 89–94.
(106) Burdett, J. K.; Albright, T. A. *Inorg. Chem.* **1979**, *18*, 2112–2120.
(107) Tolman, C. A. *Chem. Rev.* **1977**, *77*, 313–348.
(108) Seufert, K.; Bocquet, M.; Auwärter, W.; Weber-Bargioni, A.; Reichert, J.; Lorente, N.; Barth, J. V. *Nat. Chem.* **2011**, *3*, 114–119.
(109) (a) Weidenbruch, M.; Stilter, A.; Peters, K.; von Schnering, H. G. *Chem. Ber.* **1996**, *129*, 1565–1567. (b) Weidenbruch, M.; Stilter, A.; Saak, W.; Peters, K.; von Schnering, H. G. *J. Organomet. Chem.* **1998**, *560*, 125–129. (c) Braunstein, P.; Veith, M.; Blin, J.; Huch, V. *Organometallics* **2001**, *20*, 627–633. (d) Zabula, A. V.; Pape, T.; Hepp, A.; Hahn, F. E. *Dalton Trans.* **2008**, 5886–5890. (e) Cabon, Y.; Kleijn, H.; Siegler, M. A.; Spek, A. L.; Gebbink, R.; Deelman, B. J. *Dalton Trans.* **2010**, *39*, 2423–2427.
(110) Laurent, A. Low-valent group 14 metal containing ligands: Versatile building blocks for the synthesis of transition metal complexes; PhD Thesis: Saarbrücken, 2007.
(111) Barth, J. V. *Surf. Sci.* **2009**, *603*, 1533.